THESIS FOR THE DEGREE OF DOCTOR OF ENGINEERING

Novel materials for high capacity sulphur based batteries

DU-HYUN LIM

CHALMERS

Department of Physics
Chalmers University of Technology
Göteborg, Sweden 2018

Novel materials for high capacity sulphur based batteries

DU-HYUN LIM

ISBN: 978-91-7597-732-4
Doktorsavhandlingar vid Chalmers tekniska högskola
Ny serie nr: 4413
ISSN 0346-718X

Deartment of Physics
Chalmers University of Technology
SE-412 96 Göteborg
Sweden

Printed by Chalmers Reproservice
Göteborg, Sweden 2018

Novel materials for high capacity sulphur based batteries

Du-Hyun Lim
Department of Physics
Chalmers University of Technology
SE-41296 Göteborg, Sweden

Abstract

Batteries have become a vital part of our everyday lives and are used in a wide range of portable electronic devices (e.g. mobile phones, laptops, toy, and power tools). With the increased problems of environmental pollution, due to the use of fossil fuels for electric energy and transportation, there is an increased need for high capacity batteries for load levelling in renewable energy systems (wind, solar, tidal, etc.) and for electric vehicles. Li-ion batteries are currently very successful in portable applications. However, the specific capacity of current systems (< 250 mAh/g, < 120 Wh/kg), typically based on lithiated graphite anodes and metal oxide cathodes, is not sufficient for large-scale applications. In addition, there is also a need to improve battery technology in terms of price and sustainability concerning the raw of materials used. This has motivated research on next generation battery technology based on other chemistries.

One of the most promising chemistries for next generation batteries is based on the conversion of sulphur. As an example, the theoretical discharge capacity of a lithium-sulphur cell is 1675 mAh/g or 2500 Wh/kg. Sulphur can also be coupled to sodium or used in the form a metal sulphide (e.g. FeS_2), still with superior capacity compared to Li-ion technology. Considering that the active material, sulphur, has a low cost and is abundant brings also the potential for a low cost and sustainable technology. However, even though sulphur-based batteries are very promising their theoretical capacity has so far not been realised in practice in a cell with long cycle life and high charge/discharge efficiency.

In this thesis, I present new materials concepts aiming to enable next generation high capacity batteries based on the conversion of sulphur. The main target has been to improve the capacity, but the materials used have also good perspective in terms of sustainability and price. A key to improve the properties has been to tailor materials on the nanoscale. One example is the fibre-based materials prepared by electrospinning. These include carbon structures for high capacity and high rate electrodes as well as gel-polymer electrolyte membranes. The results presented in the thesis show that high discharge capacity and good cycle performance can be achieved with the new materials concepts. The functional mechanisms behind the concepts is discussed and the role of different material aspects is revealed.

KEYWORDS: next generation batteries, lithium-sulphur battery, catholyte, gel electrolyte, electrospinning

List of Publications

Paper I: Route to sustainable lithium-sulfur batteries with high practical capacity through a fluorine free polysulfide catholyte and self-standing Carbon Nanofiber membranes
D.H Lim, M. Agostini, F. Nitze, J. Manuel, J.H. Ahn, A. Matic
Scientific Reports 7, 6327 (2017),

Paper II: An electrospun nano-fibre membrane as gel-based electrolyte for room temperature Na/S batteries
D.H. Lim, M. Agostini, J.H. Ahn, A. Matic
Accepted for publication in Energy Technology (2018)

Paper III: Electrospun core-shell nanofiber web as high performance cathode for iron disulfide-based rechargeable lithium batteries
A. K. Haridas, J.E. Lim, D.H. Lim, J.K. Kim, K.K. Cho, A. Matic, J.H. Ahn
Submitted for publication, under review

Paper IV: Free-standing 3-D sponged nano-fibre electrodes for ultrahigh-rate energy storage devices
M. Agostini, D.H. Lim, S. Brutti, N. Lindahl, J.H. Ahn, B. Scrosati, A. Matic
Submitted for publication, under review

Paper V: Towards low cost and high energy lithium sulfur batteries through the use of a tailored fluorine-free Li_2S_8 based electrolyte
M. Agostini, D.H. Lim, M. Sadd, J.Y. Hwang, S. Brutti, J.H. Ahn, Y.K. Sun*, A. Matic*
Submitted for publication

Paper VI: Stabilizing the Performance of High-Capacity Sulfur Composite Electrodes by a New Gel Polymer Electrolyte Configuration
M. Agostini, D.H. Lim, C. Fasciani, M. Sadd, M.A. Navarra, S. Panero, S. Brutti, A. Matic, B. Scrosati
ChemSusChem 10, 3490 – 3496 (2017)

My contribution to appended papers

Paper I: I made all samples, performed the experiments and data analysis. I wrote the first version and together with the other co-authors finalized the paper.

Paper II: I performed the synthesis and preparation of the electrospun nano-fibre samples, the data analysis and electrochemical testing and evaluated the results. I wrote the first version and together with the other co-authors finalized the paper.

Paper III: I performed the electrochemical experiments with data analysis and evaluation. Together with the co-authors I discussed all results and participated in finalizing the paper.

Paper IV: I performed the synthesis and preparation of the CNF anode and the electrochemical testing, data analysis and evaluation. Together with the co-authors I discussed all results and wrote my part of experimental and results sections. Together with the other co-authors I participated in finalizing the paper.

Paper V: I performed the electrochemical experiments with data analysis and evaluation. Together with the co-authors I discussed all results and wrote my part of experimental and results sections. Together with the co-authors I participated in finalizing the paper.

Paper VI: I performed the electrochemical and electrolyte uptake experiments. I wrote that part of the experimental and results sections. Together with the co-authors I discussed all results and participated in finalizing the paper.

Other Publication not appended due to overlap or of out of scope.

1. Role of organic solvent addition to ionic liquid electrolytes for lithium-sulphur batteries
Shizhao Xiong, Johan Scheers, Luis Aguilera, Du-Hyun Lim, Kai Xie, Per Jacobsson, Aleksandar Matic
RSC Advances, 5, 2122 (2015)

2. Rechargeable-hybrid-seawater fuel cell
Jae-Kwang Kim, Franziska Mueller, Hyojin Kim, Dominic Bresser, Jeong-Sun Park, Du-Hyun Lim, Guk-Tae Kim, Stefano Passerini, Youngsik Kim
NPG Asia Materials 6 (2014)

3. Effect of carbon coating methods on structural characteristics and electrochemical properties of carbon-coated lithium iron phosphate
Jae-Kwang Kim, Dul-Sun Kim, Du-Hyun Lim, Aleksandar Matic, Ghanshyam S. Chauhan, Jou-Hyeon Ahn
Solid State Ionics 262, 25–29 (2014)

4. Electrochemical characterization of poly(vinylidene fluoride-co-hexafluoro propylene) based electrospun gel polymer electrolytes incorporating room temperature ionic liquids as green electrolytes for lithium batteries
Prasanth Raghavan, Xiaohui Zhao, Hyunji Choi, Du-Hyun Lim, Jae-Kwang Kim, Aleksandar Matic, Per Jacobsson, Changwoon Nah, Jou-Hyeon Ahn
Solid State Ionics 262, 77–82 (2014)

5. All Fluorine-free Lithium Battery Electrolytes
Johan Scheers, Du-Hyun Lim, Jae-Kwang Kim, Elie Paillard, Wesley A. Henderson, Patrik Johansson, Jou-Hyeon Ahn, Per Jacobsson
Journal of Power Sources 251, 451-458 (2014)

7. Ionic liquid and hybrid ionic liquid/organic electrolytes for high temperature lithium-ion battery application
Nareerat Plylahan, Manfred Kerner, Du-Hyun Lim, Aleksandar Matic, Patrik Johansson
Electrochimica Acta 216, 24–34 (2016)

8. Towards more thermally stable Li-ion battery electrolytes with salts and solvents sharing nitrile functionality
Manfred Kerner, Du-Hyun Lim, Steffen Jeschke, Tomas Rydholm, Jou-Hyeon Ahn, Johan Scheers
Journal of Power Sources 332, 204-212 (2016)

9. Coin-cell supercapacitor based on CVD grown and vertically aligned carbon nanofibers (VACNFs)
Amin M Saleem, Andrea Boschin, Du Hyun Lim, Vincent Desmaris, Patrik Johansson, Peter Enoksson
International Journal of Electrochemical Science, 12, 6653–6661 (2017)

10. Tailormade electrospun multilayer composite polymer electrolytes for high-performance lithium polymer batteries
Du-Hyun Lim, Anupriya K. Haridas, Stelbin Peter Figerez, Prasanth Raghavan, Aleksandar matic, Jou-Hyeon Ahn
Accepted for publication in Journal of Nanoscience and Nanotechnology.

Table of Contents

List of Figures

1 Introduction

We are using many different types of batteries in our everyday life, such as lithium-ion batteries (smart phone, tablet PC, laptop PC), lead-acid batteries (car), Ni-MH batteries (electric toothbrush), silver-oxide cells (watch), manganese batteries (remote control) and alkaline batteries (toys). We are also using very much energy, directly as electricity or as fuels for transportation or heating. The major part of this energy is derived from fossil resources, e.g. coal, oil, or natural gas, which results in a large release of CO_2 to the atmosphere as well as of other greenhouse gases. As a result, this environmental pollution has brought us serious global warming leading to for instance sea level rise and desertification. Large research efforts are now being dedicated to the realisation of renewable energy sources, such as wind, solar or tidal energy. However, renewable energy sources often have a serious limitation in that they are intermittent, i.e. depend on that there is for instance sunshine or wind.

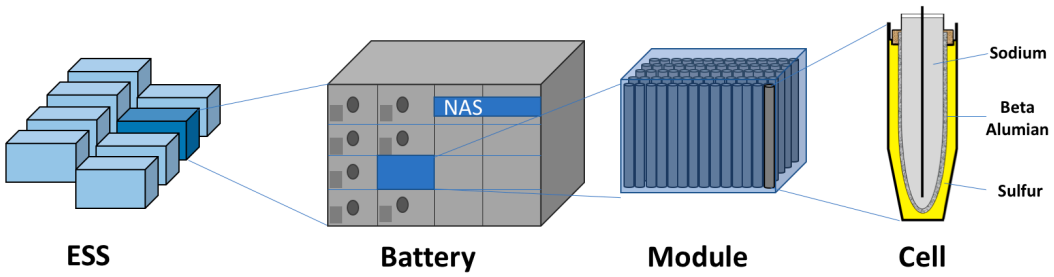

Figure 1. Energy storage system based on high temperature NaS-cells [1].

In order to address the problem of intermittent energy sources energy storage systems (ESS) are required. There are many kinds of energy storage systems that can be used, such as secondary batteries, pumping-up power generation, electric double-layer storage batteries, flywheels, superconducting energy storage, or compressed air. The secondary battery system is one of the best candidates for many applications, one example being the high temperature (over 300 °C) sodium sulphur battery used by the Japanese company NGK Insulators, Figure 1 [1]. In addition, secondary batteries are also of high interest for transportation to enable the change from gasoline or diesel fuel to electricity in electric or hybrid-electric vehicles (EVs/HEVs) [2-4]. Figure 2 shows the annual PEV (plug-in electric vehicles) sales in USA (actual and forecast) for the period 2013 to 2025. PEV sales are predicted to increase significantly and the forecast is 1.2million sold PEVs by 2025. Thus, the need for high capacity batteries is expected to increase dramatically in the coming years.

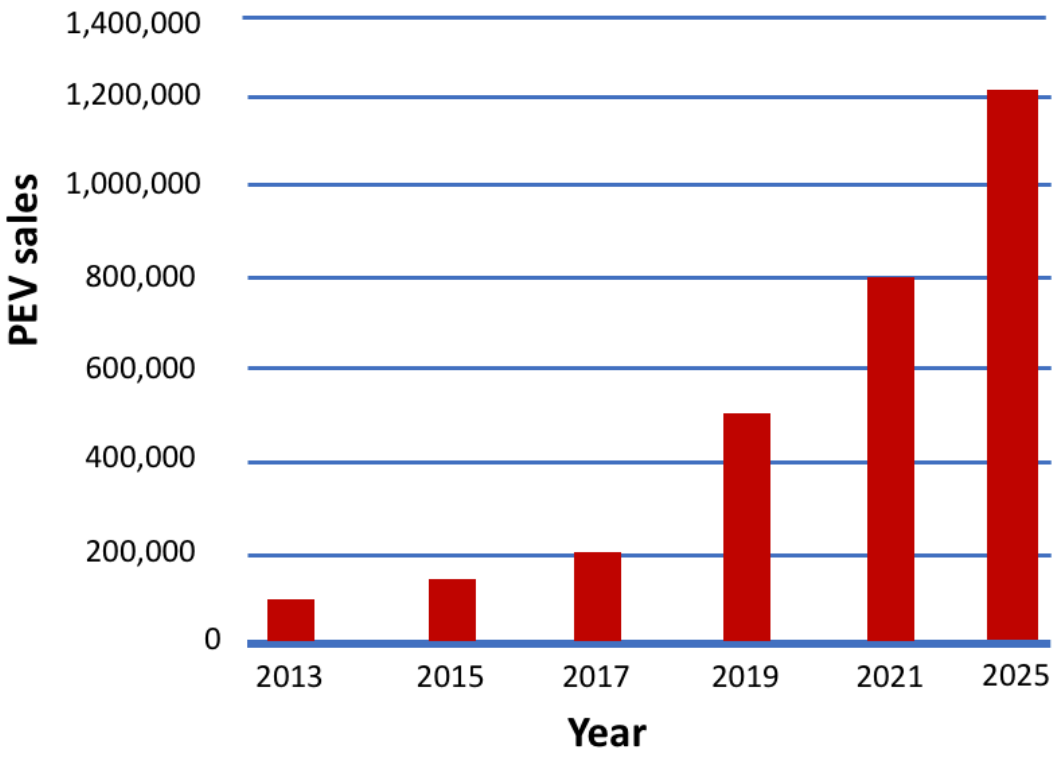

Figure 2. Annual PEV sales in USA, actual and forecast. (Data taken from HybridCars.com and insideevs.com, April 2018).

To satisfy the requirement for large-scale energy storage we need to develop the next generation of battery systems. The best technology currently is the Li-ion battery, based on a metal oxide cathode ($LiMO_2$, e.g. M=Co, Ni and Mn) and a lithiated graphite anode [5-6]. It has many advantages such as good cycle performance, high charge/discharge efficiency and high thermal stability. However, the specific capacity (< 250 mAh/g, < 120 Wh/kg) is on the limit for large-scale energy storage and the cost is also very high. The capacity is intrinsically limited by the chemistry used. Thus, one cannot achieve a step change in capacity with Li-ion technology and new chemistries and concepts need to be considered.

There are several chemistries and concepts proposed for the next generation energy storage systems with theoretical capacities superior to current Li-ion technology. The Li-sulphur battery is a very good candidate, due to a high theoretical capacity combined with the use of abundant, cheap, and non-toxic materials [7-8]. However, there are several serious problems that need to be overcome before the technology can be implemented. They are associated with bad cycle performance, low charge/discharge efficiency, and loss of active material [9-12]. In recent years, many researchers have also investigated the NaS battery system because of a high energy density (760 Wh/kg), and since both Na and S are very abundant and cheap [13]. There are already commercial NaS batteries, however operating at high temperature (> 300 ºC). These batteries do not use the full capacity available and the active materials are in the liquid state. This results in high risk of corrosion and safety problem. Thus, the challenge is to realise NaS-technology at room temperature.

In this thesis I present results on new materials concepts aimed at bringing the promising technologies based on the conversion of sulphur closer to realization. A particular focus has been on concepts with a high practical capacity, i.e. where the cell has high active material loading and not only a high specific capacity (mAh/g), and stable cycling. In addition, the concepts proposed also contribute to a lower cost and increased sustainability. One example is the cells which are fluorine free (no binders and no fluorinated salts) improving both cost and sustainability.

To reach an improved performance materials development is needed as well as an increased understanding of the connection between the properties of the materials and the processes taking place during discharge/charge. Key points have been to tailor the morphology of cathodes, anodes and electrolyte membranes to enable high loading of active material in the cell and to have fast kinetics and efficient reactions. The morphology and surface properties of the materials are also keys to prevent side reactions and to obtain high reversibility, i.e. stable cycling. Good examples are the materials prepared by electrospinning where the morphology can be tuned both through the preparation procedure as well as with post-preparation treatment, obtaining for instance different surface area and/or pore sizes. To understand the functionality of the new materials a range of experimental tools have been used to analyse the structure, composition, electrochemical properties, and in the end the performance in full cells.

2 Batteries

In a battery an active material's chemical energy is changed to electric energy through an electrochemical reaction. The battery is composed of a cathode, an electrolyte and an anode. At discharge the anode is the negative electrode and electrons leave the cell and oxidization takes place. The cathode is the positive electrode at discharge where electrons enter the cell and reduction takes place during the electrochemical reaction. The electrolyte's role is to transfer ions between the cathode and anode. The voltage of the battery is determined by the chemical potential difference between cathode and anode [14].

Batteries are commonly divided into primary and secondary batteries depending if they are non-rechargeable or rechargeable. Common primary battery types are the manganese battery, the alkaline battery, the silver-oxide cell, and the primary lithium battery. Primary batteries are suited for supplying energy for a long time and with a low current in devices such as smoke detectors, clocks, remote controls and emergency lanterns. Common secondary batteries are the lithium-ion battery, the lead-acid battery, the Ni-MH battery, and the NiCd battery. Secondary batteries are normally more expensive than primary batteries but can be economical in the long run and are today mainly used in small devices, such as smart phones, tablets, laptops and cars (Lead-acid battery). An expanding application for secondary batteries is large-scale energy storage aimed for uninterruptible power supply (UPS), electric and hybrid-electric vehicles (EVs/HEVs) and renewable energy storage. The application of batteries in our everyday life is depicted in Figure 3.

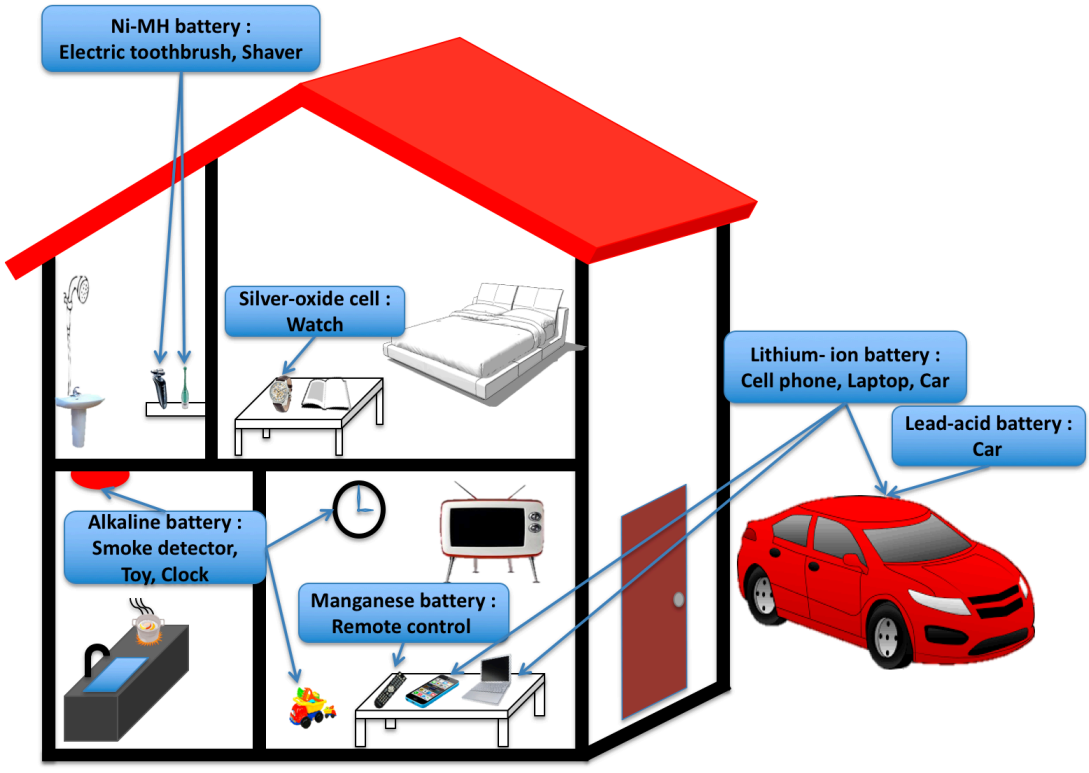

Figure 3. Batteries in our everyday life.

2.1 Li-ion batteries

The lithium-ion battery (LIB) is currently the most successful secondary battery system. It has many advantages, such as high energy density, low self-discharge and no memory effect. It is most frequently used in portable devices, but it is also being applied to HEV and EV [2-4]. Figure 4 shows a schematic picture of a Lithium-ion battery where lithium ions move from the anode to the cathode during discharge and move from the cathode to the anode during charge. Lithium metal oxides ($LiMO_2$) and lithium metal phosphates ($LiMPO_4$) are the most common cathode materials and graphite is the most common anode material in LIBs [15,16]. The Japanese company Sony was first to commercialize LIBs in 1990, using a $LiCoO_2$ cathode and a carbon anode [17]. The electrochemical reactions of a typical $LiMO_2$ cell are:

$$\begin{aligned} &\text{Cathode} && : \quad x\text{Li}^+ + x\text{e}^- + \text{Li}_{1-x}\text{MO}_2 \leftrightarrow \text{LiMO}_2 \\ &\text{Anode} && : \quad \text{Li}_x\text{C}_6 \leftrightarrow x\text{Li}^+ + x\text{e}^- + \text{C}_6 \\ &\text{Overall reaction} && : \quad \text{LiMO}_2 + \text{C}_6 \leftrightarrow \text{MO}_2 + \text{LiC}_6 \end{aligned}$$

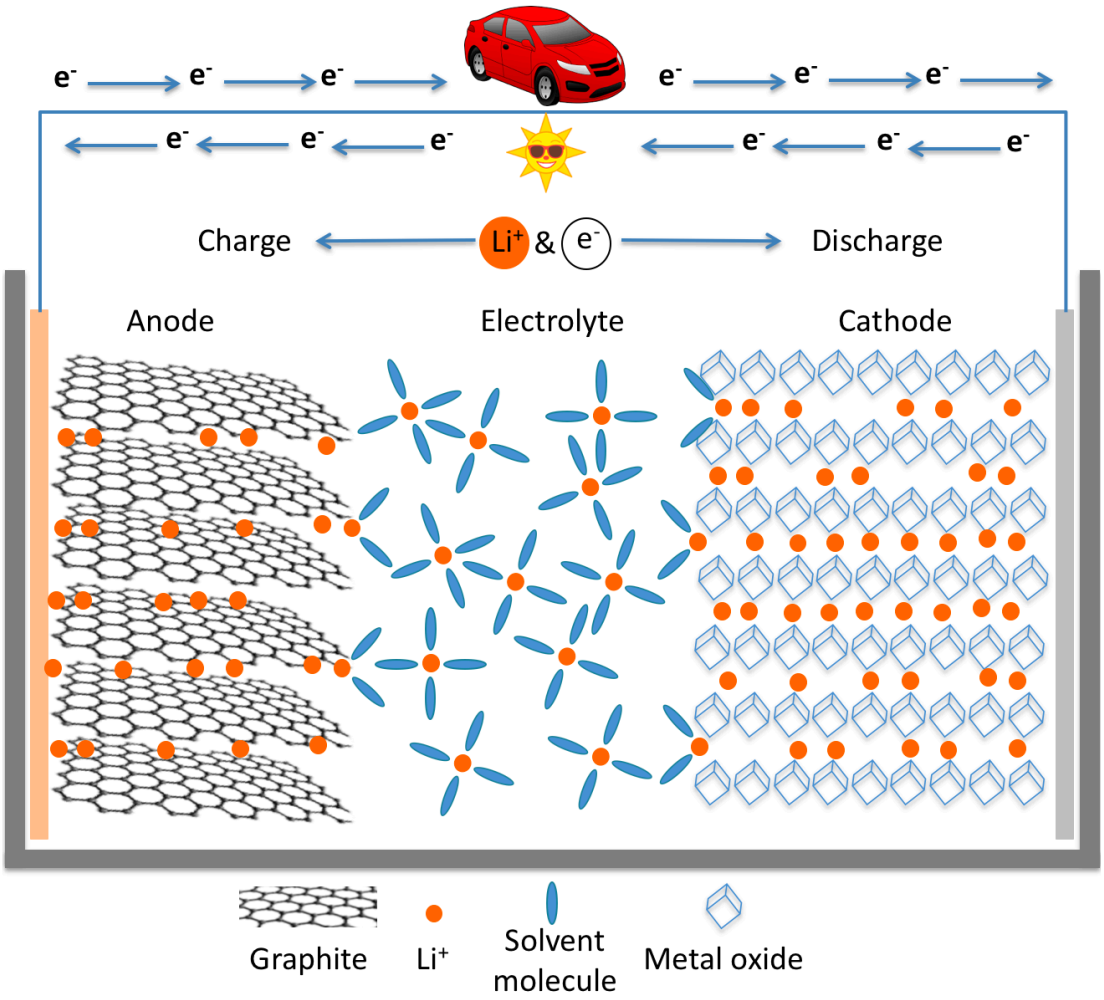

Figure 4. Schematic of a Lithium-ion battery.

$LiCoO_2$ is one of the most common cathode materials used in commercial Li-ion batteries. Li-ion insertion/extraction is very easy and reversible in this material, because of an open layered structure. The theoretical capacity of the material is 274 mAh/g, but one can only reach 120 - 155 mAh/g in practice. The origin of this difference is due to that structure expands by increased depth of charge (DOC), and there will be a structural transition at above half the DOC (at 4.2 V). In addition, Co is toxic and expensive, which has led to extensive research for new cathode materials [18-21]. One example is $LiFePO_4$ which has a stable structure, thermodynamic stability, and very good cycle performance in Li-ion cells [22]. However, $LiFePO_4$ has low theoretical capacity at high discharge/charge rates (C-rate), because of a low electronic conductivity.

Anode materials should have a standard electrode potential near that of Li metal, high capacity, cycle stability (Coulombic efficiency) and good rate capability. Li metal would be the ideal anode material for Li batteries, due to the high theoretical specific capacity (3860 mAh/g). However, there are severe problems with stability and reversibility due to lithium dendrite formation during charging, which eventually can short circuit the cell [23]. The most common anodes are instead based on Li intercalation in graphite. They have good reversibility, but a rather low theoretical specific capacity (375 mAh/g). The key to the reversibility is the formation of a stable solid electrolyte interphase (SEI) with the electrolyte. Hard and soft carbons are cheaper and have higher theoretical capacities than graphite but also high irreversible capacities during the first cycles. Soft carbon can be synthesized through thermal treatment of graphite at high temperature, whereas hard carbon can be obtained by carbonization of thermosetting plastics or organic compounds. Also oxides can be used as anodes and $Li_4Ti_5O_{12}$ (Lithium titanium oxide) is made for high-rate and long cycle life applications. $Li_4Ti_5O_{12}$ can reduce the risk of explosion and fire, because of a high thermal stability [24,25]. However, it has low theoretical specific capacity (175 mAh/g) and the energy density is low since the standard electrode potential vs $Li^+/Li°$ is 1.6 V.

The electrolyte should ideally have a high ionic conductivity, high thermal stability, wide liquid range, high electrochemical stability and, as for all battery materials, a low price. In commercial Li-ion batteries the electrolytes are based on carbonate organic solvents, such as ethylene carbonate (EC), propylene carbonate (PC), or dimethyl carbonate (DMC) [26]. The carbonates have low viscosity and high solubility for common Li-salts, e.g. $LiPF_6$, providing a high conductivity, see Table 1, and the ability to form a stable solid electrolyte interphase on the electrodes [26,27]. The disadvantage of using organic solvents are a high vapor pressure, low flash point and risk of crystallization at low temperature.

Table 1. Ionic conductivity of 1M $LiPF_6$ in different carbonate organic solvent [26].

Solvent	Ionic conductivity (mS/cm) at room temperature
EC	7.2
PC	5.8
DMC	3.1
EC/DMC (50:50 vol %)	11.6
PC/DMC (50:50 vol %)	11.0

To improve mainly safety aspects and to enable the use of metallic lithium as anode considerable efforts have been devoted to develop solid electrolytes based on polymers or ceramics combined with Li-salts [28,29]. Using a solid introduces flexibility concerning the design of the cell and also reduces the requirement on the packaging since there is no risk for leakage. The drawbacks of solid electrolytes are mainly a low conductivity at room temperature and high interfacial resistance towards the electrodes. There are examples of commercial batteries using solid polymer electrolytes, but these then operate at typically 80 °C. With gel-type electrolytes one can overcome some of the problems. In a gel-electrolyte a liquid electrolyte is confined in a polymer matrix, thus exploiting the high conductivity of the liquid phase and the mechanical stability of the polymer matrix.

Despite the success of LIBs for small scale portable applications there are limitations for their use in large-scale applications related to a limited capacity, safety issues, cost, and sustainability. With current state-of-the art Li-ion batteries one typically reaches less than 200 km driving distances of a car. This is due to a combination of a very high cost for the battery and limited energy density (< 250 mAh/g, < 120 Wh/kg). Thus, for large-scale applications there is a need for other battery technologies based on other chemistry. Many different types of battery systems are currently investing, such as Li-air, Li-S and Zn-air. Figure 5 shows the practical specific energies for different chemistries [30-33].

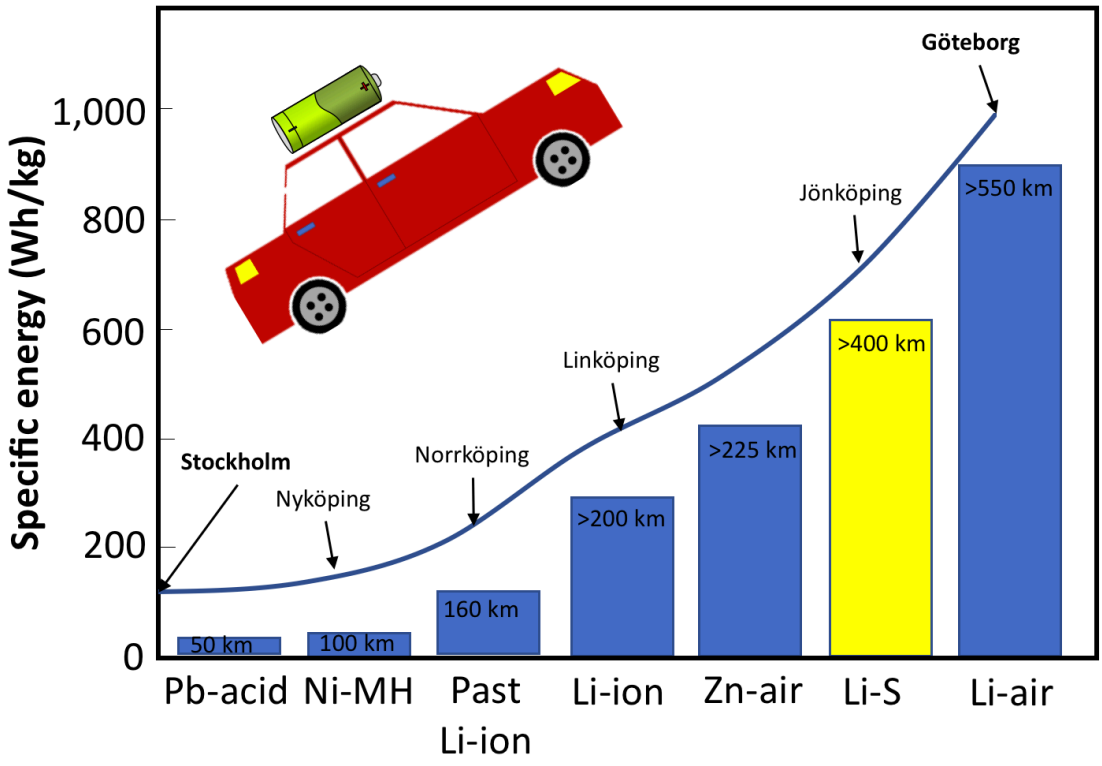

Figure 5. Specific energies for rechargeable batteries and along with estimated driving distances. (Data taken from Nature Materials 11 (2012) 19-29).

3 Sulphur Batteries

3.1 LiS battery

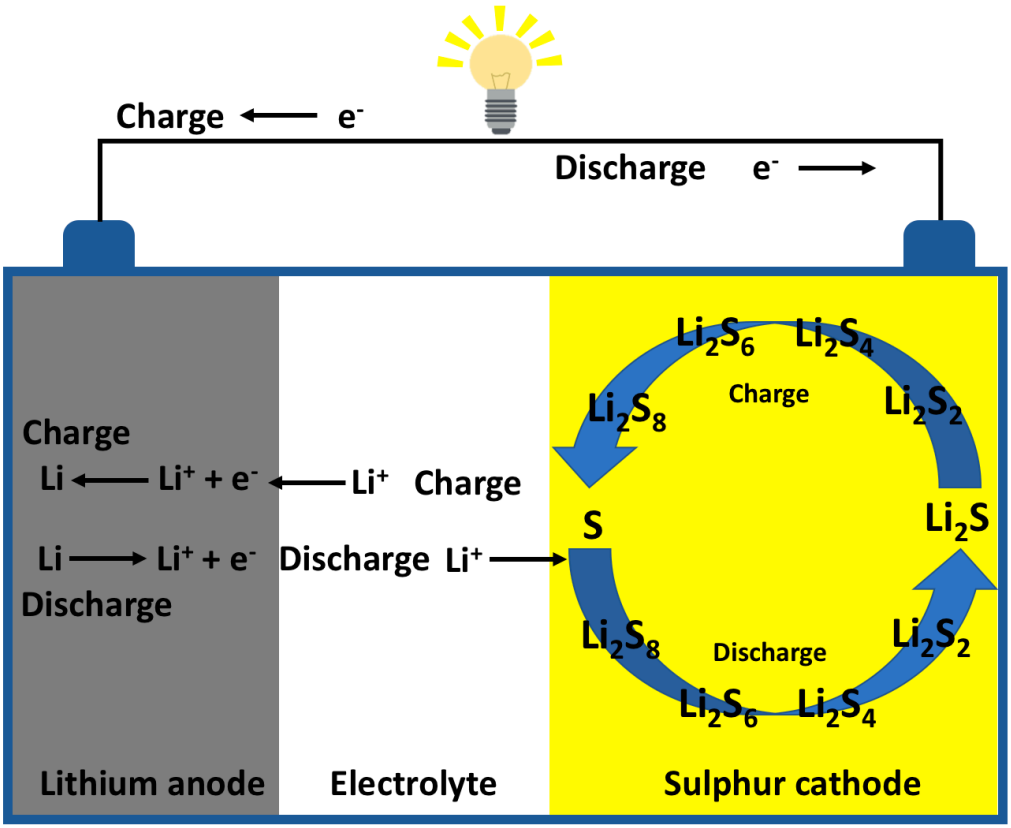

Figure 6. Schematic of an ideal Lithium-sulphur battery and principle of the charge-discharge reactions.

The Lithium-sulphur (LiS) battery is one of the most promising next generation battery concepts due to that sulphur is cheap and abundant, and in particular due to the high theoretical specific capacity, 1675 mAh/g, and energy density, 2600 Wh/kg [34-36]. Apart from the capacity and potential for sustainability the LiS-cell is safer than a LiB-cell due its intrinsic protection mechanism for overcharge, since the sulphur cathode will not change structure during overcharge.

The high capacity comes from the electrochemical conversion reaction of elemental sulphur to Li_2S. Thus, ideally the cathode is made from elemental sulphur and the anode of metallic lithium, see Figure 6. At discharge Li-ions move from the Li-anode to the S-cathode, and the ideal electrochemical reaction of a LiS-cell can be summarized as

$$S_8 + 2(Li^+ + e^{-1}) \rightarrow 2Li^+ + S_8^{-2} \rightarrow Li_2S_8 \qquad (3\text{-}1)$$

$$3/4S_8 + 2(Li^+ + e^{-1}) \rightarrow 2Li^+ + S_6^{-2} \rightarrow Li_2S_6 \qquad (3\text{-}2)$$

$$2/3S_6 + 2(Li^+ + e^{-1}) \rightarrow 2Li^+ + S_4^{-2} \rightarrow Li_2S_4 \quad (3\text{-}3)$$

$$S_4 + 4(Li^+ + e^{-1}) \rightarrow 4Li^+ + 2S_2^{-2} \rightarrow 2Li_2S_2 \quad (3\text{-}4)$$

$$S_2 + 4(Li^+ + e^{-1}) \rightarrow 4Li^+ + 2S^{-2} \rightarrow 2Li_2S \quad (3\text{-}5)$$

As a result of these reactions the discharge curve of a LiS-cell has two plateaus in the voltage profile, as shown in Figure 7, related to the different reaction steps. The first high voltage plateau, around 2.4 V, is the transformation region S → Li_2S_8 → Li_2S_6 → Li_2S_4, reactions (3-1), (3-2), and (3-3) in the scheme above. The second voltage plateau, around 2.1 V, is related to the transformation region Li_2S_4 → Li_2S_2 → Li_2S, reactions (3-4) and (3-5) in the scheme above [37,38].

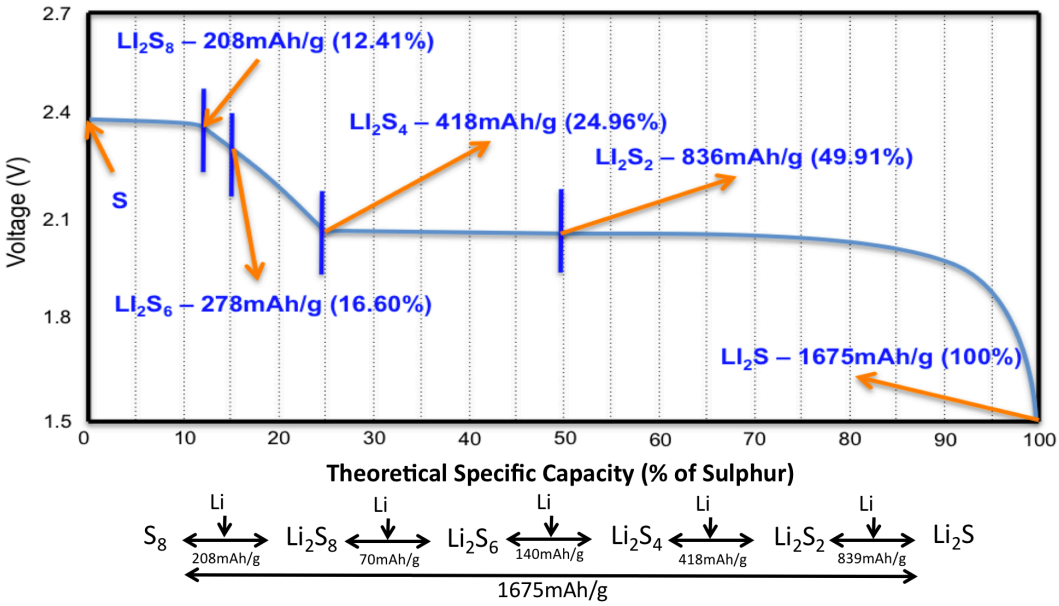

Figure 7. Schematic illustration of the discharge voltage profile of a LiS-cell and the corresponding conversion reactions.

However, in-situ x-ray diffraction [39], Raman spectroscopy [40] and UV-vis spectroscopy [41] have shown that that there is a range of other polysulphides present apart from those predicted by the ideal reactions, (3-1) to (3-5) [42]. This is a result of disproportionation reactions and the following reactions have been suggested to take place at the first (3-6) and second voltage plateaus (3-7), respectively, leading to a complicated mix of polysulphide species at the different stages [43].

$$S_8 + 2e^- \rightarrow 2S_8^{2-} \quad (3\text{-}6a)$$

$$4S_8^{2-} \rightarrow 4S_6^{2-} + S_8 \quad (3\text{-}6b)$$

$$S_6^{2-} \rightarrow 2S_3^{-} \quad (3\text{-}6c)$$

$$2S_8^{2-} \rightarrow 2S_4^{2-} + S_8 \quad (3\text{-}6d)$$

$$S_8^{2-} + S_6^{2-} \rightarrow 2S_3^{2-} + S_8 \quad (3\text{-}6e)$$

$$S_8^{2-} + 2e^- \rightarrow S_8^{4-} \quad \text{(3-7a)}$$

$$S_8^{4-} \rightarrow 2S_4^{2-} \quad \text{(3-7b)}$$

$$S_6^{2-} + 2e^- \rightarrow S_3^{4-} \quad \text{(3-7c)}$$

$$S_3^{-} + e^- \rightarrow S_3^{2-} \quad \text{(3-7d)}$$

$$2S_3^{2-} + S_6^{2-} \rightarrow 3S_4^{2-} \quad \text{(3-7e)}$$

$$3S_4^{2-} \rightarrow 2S_6^{2-} + 4S_3^{2-} \quad \text{(3-7f)}$$

LiS batteries have many advantages, but they are still not available commercially. Common problems for LiS-cells are low charge/discharge efficiency, capacity fading, low rate capability and volume change of active materiel during cycling. One of the major issues behind these problems is that the reaction products, the lithium polysulphides (Li_2S_n, $8 \geq n > 2$), are easily dissolved in the commonly used liquid electrolytes [44-46]. This leads to active material loss upon cycling and to shuttle reactions as the polysulphides can migrate to the anode side, as show in figure 8. The dissolved polysulphides increase the viscosity of the electrolyte and the resistance of the cell. Additionally, the theoretical capacity cannot be fully exploited due to the fact that sulphur has a low electronic conductivity, around $5 \cdot 10^{-30}$ S/cm at 25 °C [47,48]. Thus, a conducting agent needs to be added to the sulphur in the cathode, typically some type of carbon, to provide electronic conduction. Hence, the active material content, i.e. the sulphur content, is in most cases < 50 % of the total weight of the cathode [8-12].

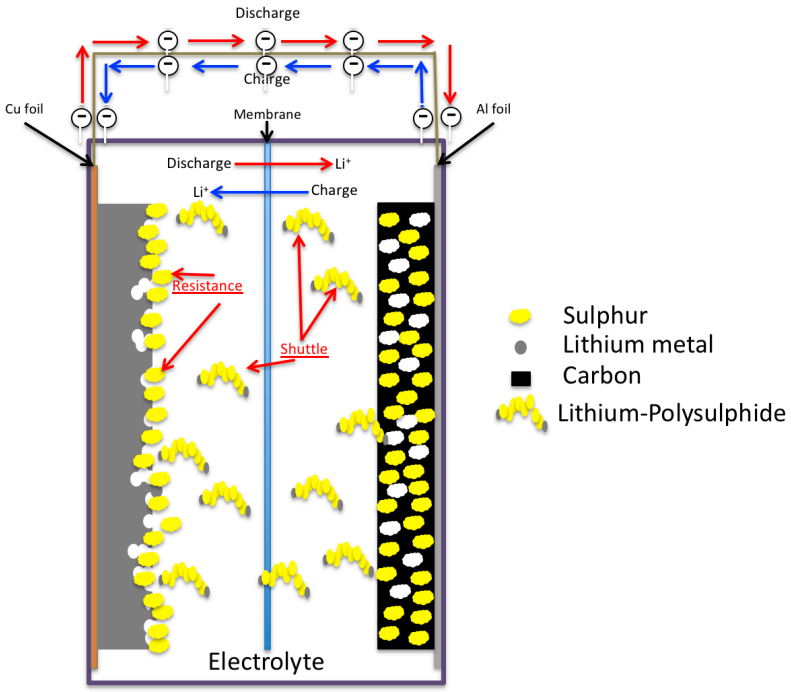

Figure 8. Potential problems in a lithium-sulphur cell.

3.1.1 Cathode materials

To address the problem of active material dissolution from the cathode and the problems associated with the shuttle mechanism several solutions have been proposed. A common approach is based on tailoring the structure of the sulphur cathode, by making carbon-sulphur composites, polyacrylonitrile (PAN)-sulphur composites, or conducting polymer coatings. In particular the work by Nazar et al provided a route for a range of new materials [49]. It is based on using mesoporous carbon (CMK-3) synthesized from a silica template (SBA-15) and the impregnation of the carbon structure by mixing sulphur and CMK-3 and heating to 155 °C, as show in figure 9. The sulphur permeates well into the porous CMK-3 structure due to its low viscosity in the liquid state at 155 °C. The idea is then that the sulphur is trapped in the in pores and that all reactions take place there. In this way lithium polysulphide dissolution can be prevented, and good cycle life, specific discharge capacity, and charge/discharge efficiency could be obtained. However, the synthesis procedure for making mesoporous carbon is complicated with many steps and loss of sulphur during heating to 155 °C can occur resulting in a low sulphur loading per weight of cathode. Recently, new porous carbon structures have been developed, such as highly porous carbon sphere (HPC) [50], hard carbon spherules-sulphur electrode (HCS-S) [51] and hollow carbon fibres [52]. These have high specific capacity (> 900 mAh/g) and good cycle stability, but low sulphur content (< 53 %) and low loading (< 2.5 mg/cm^2).

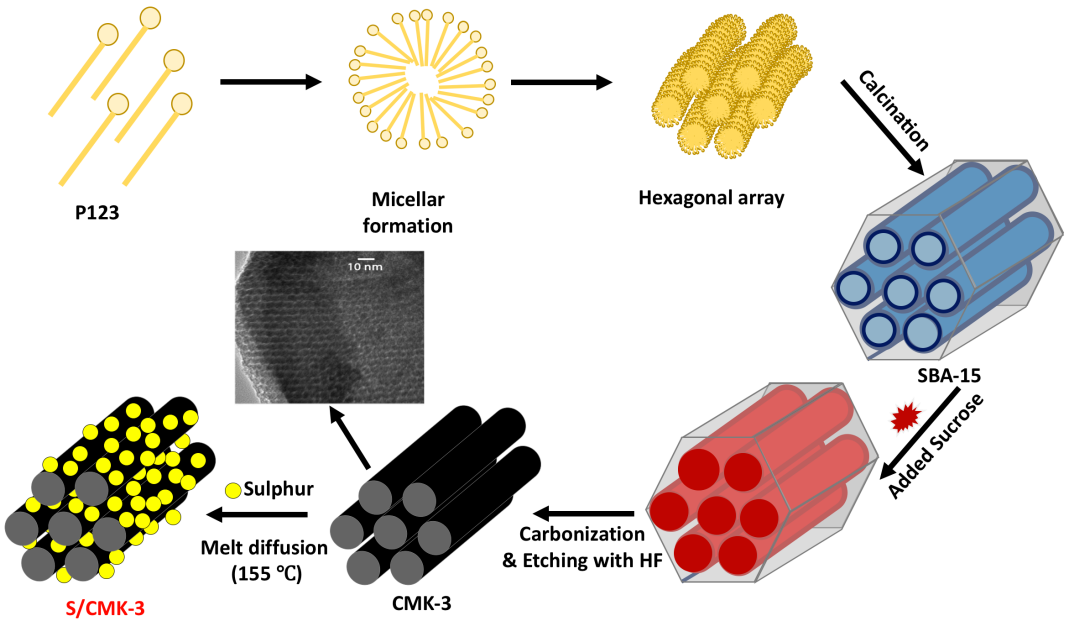

Figure 9. Schematic synthesis of the CMK-3 ordered mesoporous carbon and the S/CMK-3 composite.

A second approach exploits coating the surface of sulphur nano-particles, with conducting polymers such as polyaniline, and polypyrrole [53-55]. It is a very similar strategy to the carbon-sulphur composite and the problems are also similar. The addition of the conducting polymer coating will both entrap the sulphur and improve the conductivity. A related strategy is a PAN-sulphur composite, introduced by Wang et al in 2003 [52]. There PAN powder and sulphur are mixed and heated to 280 - 300 °C. This induces a reaction where the –CN and –CH_2 groups of the polymer are replaced

by C=C and –CH groups of cyclic structures and the sulphur is trapped in the structure, as shown in Figure 10 [56,57]. The discharge curve for this cathode has a different profile, not showing the two plateaus at 2.4 and 2.1 V, but instead one plateau at a lower voltage (2.1 - 1.5V). The system also shows different cycling performance in the first and second cycle, but overall it has a good cycle life and high specific discharge capacity. An advantage of this approach is that the cathode is compatible with carbonate-based electrolytes, which are cheap, in contrast to other cathode materials that have bad cycle life using carbonate electrolytes. However, the lower working voltage of the PAN-sulphur composite is a serious drawback in addition to the common problem of the other approaches with the limited sulphur loading (40 %) in the cathode, which decreases the practical energy density [57].

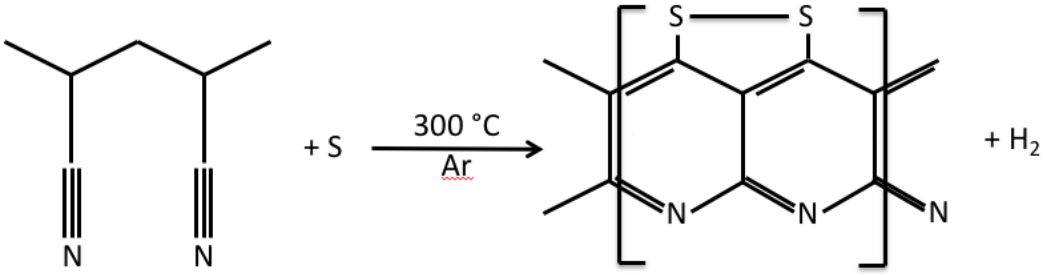

Figure 10. Schematic illustration of chemical transformation of PAN and sulphur at 300 °C [56,57].

3.1.2 Electrolytes

For the functionality of a LiS-cell the electrolyte is as important as the cathode. In addition to providing fast ion transport it has also to be compatible with the carbon structures in the cathode and plays as central role concerning polysulphide dissolution. If the solubility of sulphur and polysulphides is high there is a risk for active material loss and side reactions at the anode through the shuttle mechanism. If the solubility on the other hand is very low then the cycling can be very stable but the utilisation of active material is generally low since all reactions take place in solid state and the kinetics are usually slow. Thus, such electrolytes are also not compatible with high active materials loading which is necessary for a high energy density in practice.

Liquid electrolytes are most commonly used in LiS-cells. However, the ordinary carbonate solvents used in Li-ion batteries usually show bad cycle performance, since the polysulphides are extremely reactive with carbonate organic solvents [58,59]. Instead, mixtures of glyme based solvents, e.g. tetraethylene glycol dimethyl ether (TEGDME), dimethoxy ethane (DME) and dioxolane (DOL or DIOX) are commonly used. Overall, the glyme based solvents have a high solubility of polysulphides and fast reaction kinetics, but this also leads to problems of the shuttle mechanism and increased resistance of the electrolyte during cycling. To mitigate these drawbacks DOL is commonly added as a second solvent since it has a low viscosity and a lower solubility for polysulphides [60].

Since it in any case is virtually impossible to totally prevent some polysulphides to be present in the liquid electrolytes it is vital in order to protect the Li-metal anode by the formation of a stable SEI. A common strategy is to add $LiNO_3$ to the electrolyte solution since it has been shown to facilitate the formation of a stable SEI on Li-metal [58-60] by the formation of a passivation layer with NO_3^- [61]. However, one has to take care so that one does not have a further decomposition of NO_3^- to NO_2 or NO_2^- and Li_2O, (3-8) and (3-9), which occurs at 1.71 V [62]. Thus, the voltage widow of cycling when using $LiNO_3$ as an additive has to be limited.

$$NO_3^- + e^- + 2Li^+ \rightarrow NO_2 + Li_2O \qquad (3\text{-}8)$$

$$NO_3^- + 2e^- + 2Li^+ \rightarrow NO_2^- + Li_2O \qquad (3\text{-}9)$$

Also ionic liquids have been considered as electrolytes for LiS-batteries. Ionic liquids are room temperature molten salts and have many attractive properties for application as electrolytes for Li batteries, such as high thermal stability, very low vapour pressure, non-flammability, high ionic conductivity and a wide electrochemical window [63-65]. Ionic liquids usually have a very low solubility for polysulphides and LiS-cells with ionic liquid electrolytes can show very stable cycling. However, the active materials utilisation is generally low and the high viscosity of ILs result in a poor rate capability. To improve the performance, mixtures of ionic liquids and organic solvents have been investigated [66,67]. Compared to neat organic solvents the presences of the ionic liquid improves the safety in terms of an increased flash point of the electrolyte. Ionic liquids have also been shown to be able to create a stable SEI on Li-anodes which is of importance for stable cycling [66].

In addition to side reactions due to polysulphide shuttles, dendrite growth is a serious problem when using Li-metal anodes. To address this problem research has been devoted to the use of solid electrolytes which can provide a physical barrier that hinders short cuts due to dendrites. Several groups have applied ceramic membranes based on Li_2S-P_2S_5 to room temperature LiS-cells [28,29]. The ceramic electrolytes can have a good ionic conductivity but the average voltage of the cell is usually low (2.0 V) which decreases the energy density. Another approach is using solid polymer electrolytes based on blends of polyethylene oxide (PEO) and Li-salts [68]. As in the case of Li-ion batteries these membranes usually have a too low conductivity at room temperature and the operational temperature of the cells has to be increased to around 70-80 °C to obtain good performance.

3.1.3 The Polysulphide Catholyte Concept

A recent approach to address the polysulphide dissolution has been to deliberately include polysulphides in the electrolyte as a buffering mechanism [23,70-74]. In addition to prevent polysulphide dissolution the added sulphur can also be electrochemically active and contribute to the capacity. Thus, the polysulphide catholyte is a very promising route to improve both the energy density and the cyclability of the systems [71,75-78]. However, problems related to the shuttle mechanism remain and are even emphasised by the high concentration of polysulphides. This makes it necessary to in some way stabilise the interface on the Li-anode to prevent

side reactions. To address these problems approaches based on the formation of a stable solid electrolyte interphase (SEI) layer using $LiNO_3$, as discussed above, has shown good results. The addition of polysulphides to the electrolyte also increases the viscosity of the electrolyte. By using low viscosity solvents, e.g. 1,3-Dioxolane (DIOX), a reasonable viscosity can be obtained even at high polysulphide concentration [79-81].

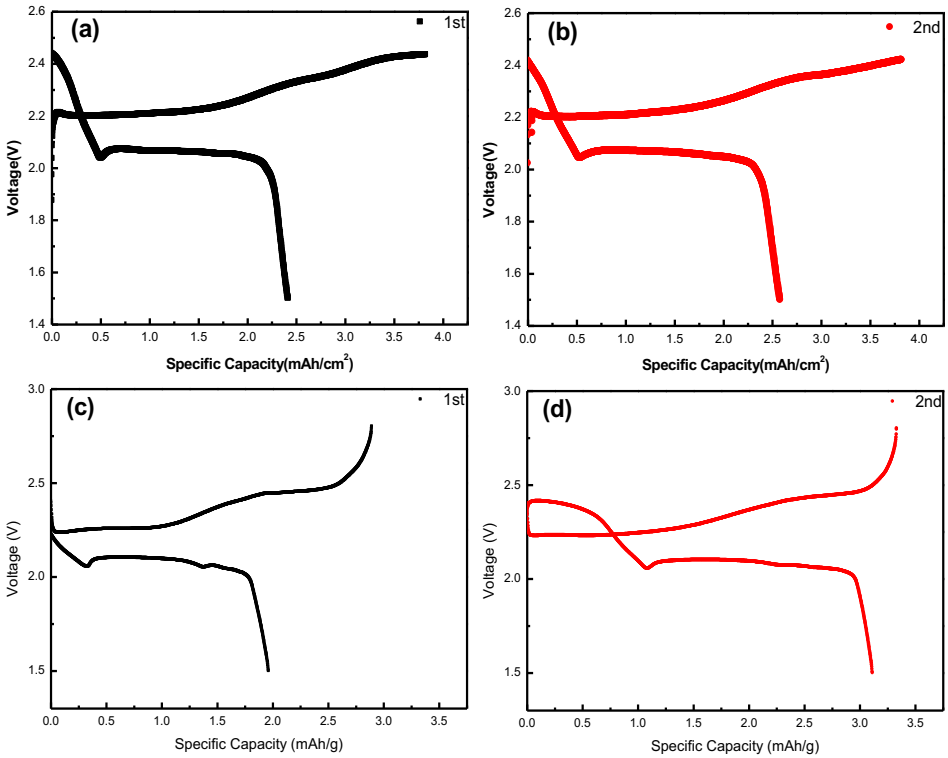

Figure 11. Discharge/charge voltage profiles of first cycle (a), second cycle (b) using an electrolyte without $LiNO_3$, and first cycle (C) and second cycle (d) using an electrolyte with $LiNO_3$.

A lithium polysulphide catholyte cell shows a different voltage profile during the first discharge behaviour compared to a standard LiS-cells. In Figure 11 discharge/charge curves for two catholyte cells, with and without the addition of $LiNO_3$, are shown. Since the starting material is Li_2S_8 one only observes the second voltage plateau (2.1 V) at first discharge. One can also see that the first charge in figure 11 (a) ends in a flat plateau, i.e. the cell could not be fully charged which is a signature of polysulphide redox shuttle reactions [46]. In Figure 11 (c), where $LiNO_3$ has been added to the catholyte one can see that full charge can be achieved, since $LiNO_3$ inhibits the shuttle mechanism. As a result, the second discharge, figure 11 (d), has two plateaus (at 2.3 and 2.1 V) in contrast to the behaviour found in figure 11 (b) where only one plateau is found also in the second discharge. This is because sulphur is the reaction product after full charge and Li_2S_8 is the reaction product after an incomplete charge in the case of an electrolyte without $LiNO_3$. As an alternative to using $LiNO_3$ nano-porous membranes have been applied to catholyte cells [82]. Membranes with pore sizes of less than 1 nm have been prepared preventing the crossover of polysulphides and thus the shuttle reactions.

3.1.4 Reaching a high practical capacity

Many papers reporting very high specific capacities (mAh/g with respect to the amount of sulphur in the cell) have quite low active material (sulphur) loading. The sulphur utilization can be very high leading to a high specific capacity but the actual energy density of the cell is usually still quite low. Table 2 compares the performance of some concepts reported in literature and one can see that many of them show an areal capacity (mAh/cm^2 reflecting better the loading and actual energy density) around 1-3 mAh/cm^2. This is actually a comparable, or lower, capacity than that of commercial state-of-the-art Li-ion batteries. With the catholyte concept a very high loading can be obtained and it is in principle only limited by the solubility of polysulphides in the electrolyte.

Table 2. Comparison of different concepts for LiS-cells [50,72,83-87].

Reference	Method	Cathode loading (mg/cm^2)	Sulphur (%)	Sulphur loading (mg/cm^2)	C-rate	Current Density (µA/cm^2)	1st cycle discharge	
							mAh/g	mAh/cm^2
Materials Research Bulletin 58 (2014) 199–203	Carbon-sulphur composite	1.5	41.04	0.62	0.1	103.9	1375	1.04
J. Mater. Chem. A, 2014, 2, 7265	Carbon-sulphur composite	2.12	47.2	1.0 (0.6-1.0)	0.1	167.5	1300	1.3
Adv. Mater. 2013, 25, 6547–6553	Carbon-sulphur composite with Pt	1.0	81	0.81	0.1	134	1283	1.04
J. Mater. Chem. A, 2013, 1, 295	PAN-sulphur composite	4	38.5	1.54	0.1	258	1223	1.88
Journal of Power Sources 265 (2014) 14	Catholyte	0.8	0	3.20 - in catholyte	0.066 (110 mA/g)	210	750	2.4
Scientific Reports 7(2017) 6327 (Paper I)	Catholyte	2.5	0	6.5 - in catholyte	0.026	250	1200	7
					0.2	2000	514	3
Scientific Reports 6 (2016) 39615	Graphene oxide aerogel	7.25	67	4.9	0.1	820	838	4.2
ACS Energy Lett. 3 (2018)72	Polysulphur graphene nano composites	15	70	10.5	0.05	879	1135	12
					0.2	3517	827	8.7

In addition, the amount of electrolyte used in the cell is also of high importance. A large amount of electrolyte will usually lead to better performance but also increases the weight. As an example, in a standard sulphur/carbon composite cathode the content of the different components is usually: 60% sulphur, 30% super-P and 10% PVdF (binder). In a cell with a quite low amount of electrolyte (10 µl/cm^2) the weight of the components would typically be: cathode 4 mg/cm^2 (sulphur loading is then 2.4 mg/cm^2), separator membrane 1 mg/cm^2, electrolyte 10 mg/cm^2, Al current collector 4 mg/cm^2, Li-metal 8 mg/cm^2, adding up to a total weight of 27 mg/cm^2. Thus, sulphur and electrolyte content are in this case 8.9 % and 37 %, respectively [69]. In many reports

in literature the electrolyte content will be between 5-20 times higher than in this example clearly showing that those cells will not be able to have a high energy density in the end and that those concepts can hardly be commercialized.

Since all active material in the catholyte concept is present in the liquid electrolyte the cathode is just a support for the electrochemical reactions. This brings some flexibility to the design of the cathode and a particularly interesting direction is to use self-supporting carbon structures. These can combine a high surface area and a high electronic conductivity to promote efficiently the electrochemical reactions. In addition, this does then also omit the need for a meal current collector, thereby further increasing the energy density of the cell [72,88].

3.2 Sodium-Sulphur Batteries

A further step to improve the sustainability can be taken by going from Li to Na as electrochemically active species. Na is considerably more abundant and cheaper than Li [89], and a NaS battery will help to provide a cheaper and more environmental friendly energy storage system. The theoretical specific capacity of the electrochemical reaction between Na and S is the same as in the case of a LiS-cells, 1675 mA/g with respect to sulphur. However, the theoretical energy density is lower due to the increased weigh of Na-metal with respect to Li (Na-1170 mAh/g, Li-3860 mAh/g).

Commercial NaS batteries already exist and are used as large-scale energy storage in power systems. However, these batteries operate at high temperature, > 300 °C. The high temperature NaS battery has a sodium anode, a sulphur cathode and a solid beta-alumina (β-Al_2O_3) electrolyte, as shown in Figure 12. At this temperature both Na and S are in the liquid phase and the conductivity of β-Al_2O_3 is high. However, the high temperature NaS battery has some serious disadvantages. These are related to corrosion by sodium polysulphides at the high temperature, risk of leakage and potential explosion of highly reactive molten sodium and increased operating cost. In addition, the capacity is limited since the cell is only discharged to the formation of Na_2S_3 resulting in a theoretical specific discharge capacity of 558 mAh/g. The reason for this is that the shorter polysulphide species, Na_2S_2 and Na_2S have higher melting points, 475 and 1175°C respectively, and would thus be solid [90]. Thus, the discharge profile only shows one plateau, as shown in Figure 13.

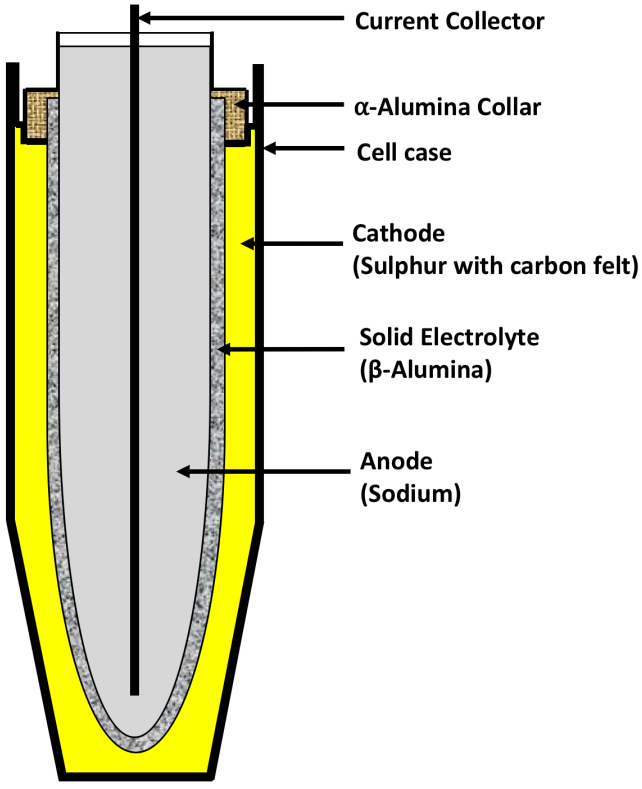

Figure 12. Schematic illustration of high temperature NaS-cell.

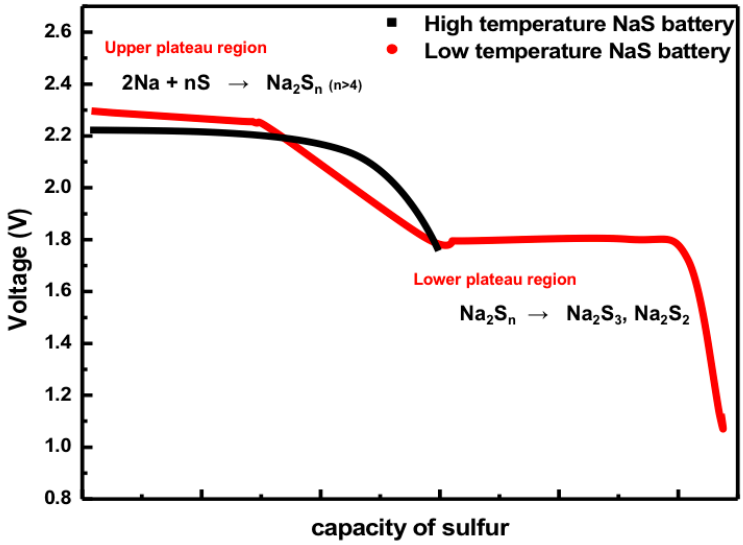

Figure 13. Schematic illustration of discharge voltage profiles of high temperature and low temperature NaS-cell, respectively.

To overcome the problems with corrosion and safety it is desirable to realise a room temperature NaS-cell. In this case both electrodes would be solid, just as in the case of the LiS-cells described above, and the specific capacity would be that of sulphur, 1675 mAh/g. The corresponding discharge profile is shown in Figure 13 and exhibits two plateaus as in the case of the LiS-cell. However, so far, the success with room temperature NaS-cells has been very limited [91-93]. The main reason is, as in the case of LiS-cells, that the intermediate reaction products, the sodium polysulphides (Na_2S_x, $x \geq 2$), are soluble in the electrolyte leading to active material loss and side reactions due to shuttle mechanisms. In the case of LiS-cells the Li-metal anode can be stabilised by the presence of $LiNO_3$ in the electrolyte. This strategy has so far not proven to be successful in the case of Na-metal electrodes, as it seems that $NaNO_3$ cannot make an SEI layer on the sodium metal anode surface. Several groups have tried to address the problem by instead using e.g. ceramic filters [94] or Na_3PS_4 solid electrolytes [95]. With these approaches a rather high specific discharge capacity has been obtained (>1000 mAh/g) but not for very many cycles and only at low C-rates. Furthermore, the sulphur content in the electrode was rather low (27 %) resulting in a low sulphur loading of the cathode (0.3 mg/cm^2).

3.3 Li/FeS_2 battery

An alternative to use elemental sulphur as active material in the cathode is to use metal sulphides [96-100]. A particularly interesting material is FeS_2 owning to a low cost, high abundance of elements and a higher electronic conductivity compared to sulphur [101,102]. When using FeS_2 as active cathode material in a Li/FeS_2 cell the theoretical energy density is ~1313 Wh/kg and the specific capacity is 894 mAh/g [103]. Despite the very promising theoretical properties, Li/FeS_2 cells developed so far suffer from poor reversibility and short cycle life. This is related to slow kinetics of the reactions, that the polysulphides created during the electrochemical processes are soluble in the electrolyte and very large volume changes.

According to Rosamad et al. [104], there are two reaction steps in the cathodic process. In the first step FeS_2 is reduced to Li_2FeS_2, and in the second step Li_2FeS_2 is reduced to Fe and Li_2S:

$2Li + FeS_2 \rightarrow Li_2FeS_2$ (4-1)

Oxidation of Iron(II) sulphide: $FeS_2 + 2e^- \rightarrow FeS_2^{-2}$

Reduction of lithium: $2Li \rightarrow 2Li^+ + 2e^-$

$Li_2FeS_2 + 2Li \rightarrow Fe + 2Li_2S$ (4-2)

Oxidation of iron: $Fe^{+2} + 2e^- \rightarrow Fe$

Reduction of lithium: $2Li \rightarrow 2Li^+ + 2e^-$

Figure 14 shows the charge/discharge profiles of a Li/FeS_2 cell. During first discharge the voltage profile is distinctly different form that of a LiS-cell, showing only one plateau around 1.5 V. However, already the first charge and subsequent discharge cycles show two plateaus, more reminiscent of a LiS-cell. This underlines that the ideal reaction is not followed and the reason is that the reactions (4-1) and (4-2) are only fully reversible at high temperatures, due to slow kinetics [105]. At ambient conditions a more complicated scheme has been proposed where during charge elemental sulphur is also created, in particular when the cell is charge to high potentials:

$2Li_2S + Fe \rightarrow Li_2FeS_2 + 2\ Li^+ + 2e$ (4-3)

$Li_2FeS_2 \rightarrow Li_{2-x}FeS_2 + x\ Li^+ + x\ e^-\quad (0 \leq x \leq 0.8)$ (4-4)

$Li_{2-}\ x\ FeS_2 \rightarrow FeS_y + (2 - y)\ S + (2 - x)\ Li^+ + (2 - x)\ e^-$ (4-5)

In Figure 14 the second and third discharge cycle in fact show a behaviour which is a mix of the discharge curve of Li/FeS_2 and Li/S. A sloping plateau is found around 2.1 V and a second plateau around 1.5 V.

Considering the electrochemical reaction mechanism outlined in (4-3) - (4-5) one can realise that polysulphide dissolution will be a severe problem also in Li/FeS_2 cells. In addition, a continuous aggregation of Fe particles upon cycling limits the reversibility of the reaction [106,107]. Several approaches have been taken to address these issues,

e.g. carbon composites using reduced graphene oxide (RGO) [108] or resilient carbon encapsulation (FeS_2@RC) using hydrothermal polymerization of glucose [109]. These concepts have high initial specific discharge capacity (> 800 mAh/g), but have a low active materials content (< 52%) in the cathode, and FeS_2@RC composite has low cycle stability.

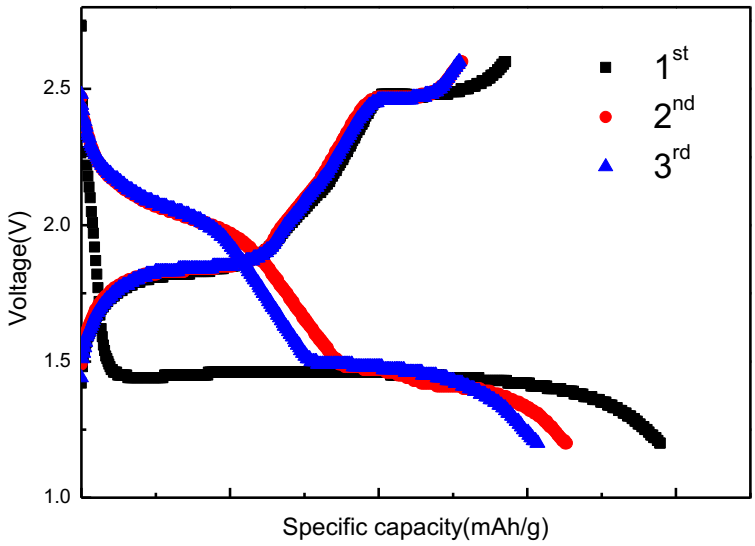

Figure 14. Charge-discharge profiles of a Li/FeS_2 cell.

4 Materials and Experimental

In this section I describe some of the experimental methods used in this thesis work. For materials preparation electrospinning is the most central method and was used for both electrodes and electrolyte membranes. To analyse the physical and electrochemical properties of the materials a wide range of methods has been applied. In this chapter I focus mostly on the description of the electrochemical methods since they are of importance to evaluate the performance.

4.1 Electrospinning and Carbonization of PAN

Several of the materials developed and applied in this thesis work were prepared through electrospinning. Electrospinning has many advantages. It is rather easy to obtain fibre-based membranes of different materials (polymers, carbon, metals and ceramics) starting from electrospinning. By tuning the processing conditions the fibre diameter, (nm to µm), surface area, and density can be varied. Thanks, to the ease of preparation, the possibility to use different materials, and to obtain different properties electrospun nano- and micro-fibres have been applied in various fields, such as separation filters, protective clothing, biomedical engineering, and as conductive fibres [110-113].

Figure 15 shows a schematic of an electrospinning setup. A polymer solution (or polymer melt) is fed through a nozzle and drawn to a fibre by a DC field applied between the nozzle and a collector. By moving the nozzle and/or using a rotating drum as collector a membrane can be formed. Even though the equipment used for electrospinning is rather simple, see figure 15, there are many process parameters to control to obtain reproducible results, e.g. electric field strength, nozzle size, distance between collector and needle, viscosity of the solution and flow rate. In addition, one needs to also consider the temperature and the humidity during preparation.

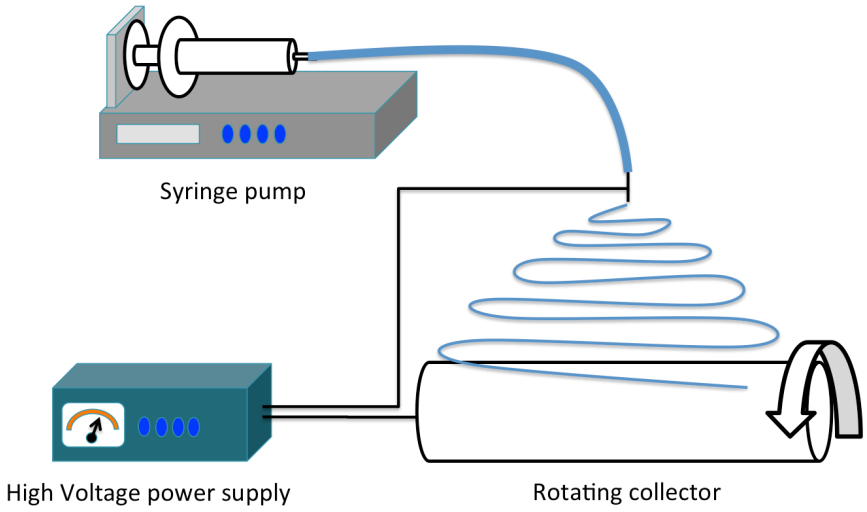

Figure 15. Schematic of an electrospinning device.

For battery applications electrospun polymer membranes have been used to form gel-type electrolyte membranes or as precursors for carbon based electrodes (see further below). Electrospun PVdF-HFP membranes (polyvinylidene fluoride-co-hexafluoropropylene) have been prepared and swollen with high viscosity liquid electrolytes (for instance based on ionic liquids or PEGDME) [67,114-115]. The morphology of the membranes, important for liquid uptake and retention, has also been further modified by the addition of nano-sized ceramic fillers ($BaTiO_3$, SiO_2, or Al_2O_3) to the polymer solution during electrospinning and thus incorporated into the fibre structure [116].

In this work electrospinning was used for the preparation of PAN nano-fibre membranes. In a typical run, a 12 wt.% polymer solution was prepared by dissolving PAN in N,N-dimethyl formamide (DMF). The polymer solution was fed through a capillary using a syringe pump and a fibrous membrane, obtained using a voltage of 20 kV, was collected on an aluminium foil fixed on a grounded stainless steel rotating drum. PAN based membranes generally have good mechanical properties since PAN is a rigid thermoplastic polymer. It is resistant to most solvents and chemicals and burns slowly. Therefore, it is a suitable material for battery application. As a precursor material for carbon fibres the molecular structure is suitable, like honeycomb, in order to make high quality carbon just by heating.

4.1.1 Carbon Nano-fibre membranes

Carbon nano-fibre membranes can be obtained by carbonization of a polymer nano-fibre membrane, in our work PAN. Figure 16 shows the reaction of PAN during carbonization. The PAN membrane is first stabilized in an oven at 250 °C for 1 h in air and then carbonized by heating in a tube furnace from room temperature to 1000 °C (heating rate of 10 °C/min), and then maintained at 1000 °C for 1 h in nitrogen (N_2) flow (800 mL/min). In the stabilization step the –CN and $–CH_2$ groups of the polymer are replaced by C=O and –CH groups of cyclic structures. In the carbonization step the oxygen and hydrogen on the C=O and –CH groups are replaced by C=C in a ladder-like structure [117,118]. However, it is usually very difficult to obtain complete carbonization of PAN [119]. Thus, the carbon nano-fibre membrane produced in this way will still contain some nitrogen and hydrogen, but normally at low concentration [119].

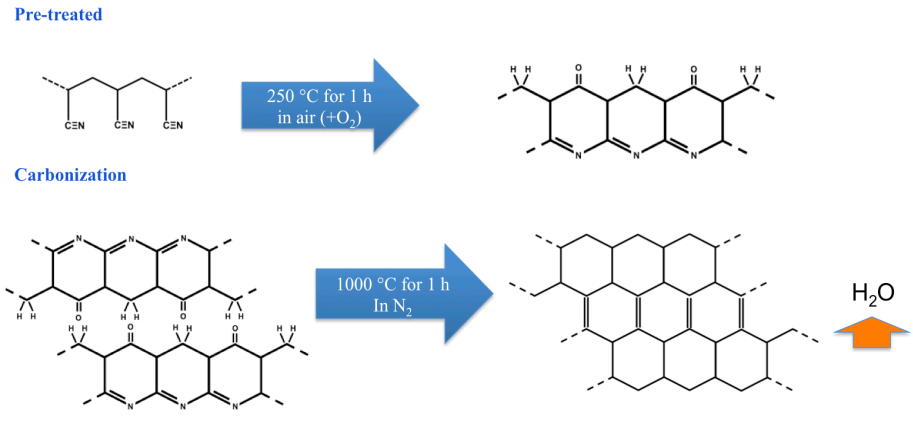

Figure 16. Chemical reaction of PAN during stabilization and carbonization.

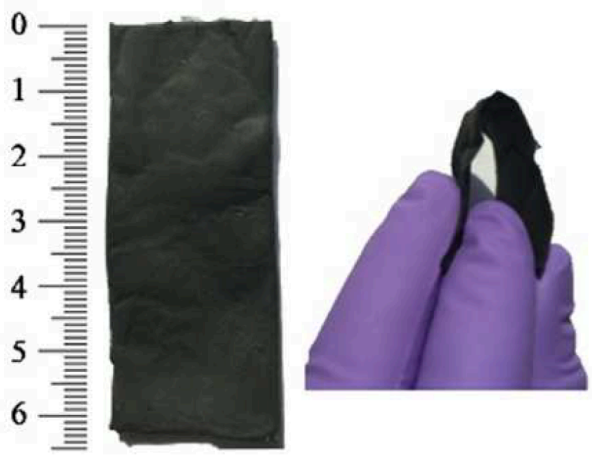

Figure 17. Self-standing carbon nano-fibre membrane prepared by electrospinning a PAN membrane followed by carbonization.

CNF membranes prepared by carbonisation of polymer precursor membranes will have uniform fibre diameter and are normally soft and flexible, see figures 17 and 18. The surface area of the membrane can be increased by chemical treatment, such as KOH etching and heat treatment, which produces small pores (few nm) in the fibres [120]. In a first step the CNF membranes are kept in a KOH solution where the following reaction takes place

$$6KOH + 2C \rightarrow 2K + 3H_2 + 2K_2CO_3.$$

In a second step the membrane is kept at high temperature (typically 750°C) inducing the following reactions.

$$K_2CO_3 \rightarrow K_2O + CO_2$$
$$CO_2 + C \rightarrow 2CO$$
$$K_2CO_3 + 2C \rightarrow 2K + 3CO$$
$$C + K_2O \rightarrow 2K + CO$$

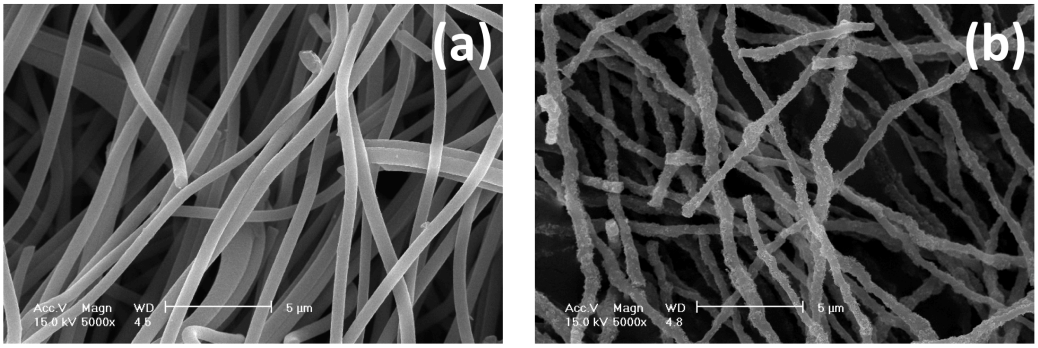

Figure 18. SEM images of the (a) pristine CNF, (b) CNF/SiO_2-HF-KOH membranes, respectively.

Figure18 shows Scanning Electron Microscopy (SEM) images of two CNF membranes. The pristine membrane, i.e. just after carbonisation, has smooth fibres with a uniform diameter. In contrast the membrane that has undergone the KOH-etching treatment has fibres with a very rough surface. In this case the morphology of the fibres has also been modified by the addition of SiO_2 nano-particles which were incorporated in the fibres during electrospinning and then etched away by HF after carbonisation. In this way larger pores are created in the fibres, roughly of the same size as the nano-particles (in our work around 20-30 nm).

There are also other methods that can be used to tune the surface area of carbon nano-fibre membranes. In literature there are examples of using added polymers (polystyrene, polymethyl methacrylate) [121,122], CO_2 treatment [123], or microwave plasma enhanced chemical vapour deposition (MPECVD) [124]. All these methods can produce membranes with high surface area (< 1320 m^2/g). In the case of MPECVD an additional layer of "carbon" species is added on top of the CNF. Compared to these methods, KOH treatment is rather simple and cheap.

4.2 Electrochemical Analysis

4.2.1 Cell assembly

In this work different types of cell geometries have been used, such as coin, pouch and Swagelok cells for electrochemical analysis. The coin and Swagelok cells are typical for laboratory scale batteries, where the amount of material is limited. The Swagelok cell is suitable to use when one wants to perform post-operational analysis of the materials in the cell. It can easily be opened and the materials can be analysed after cycling and the cell can be reused.

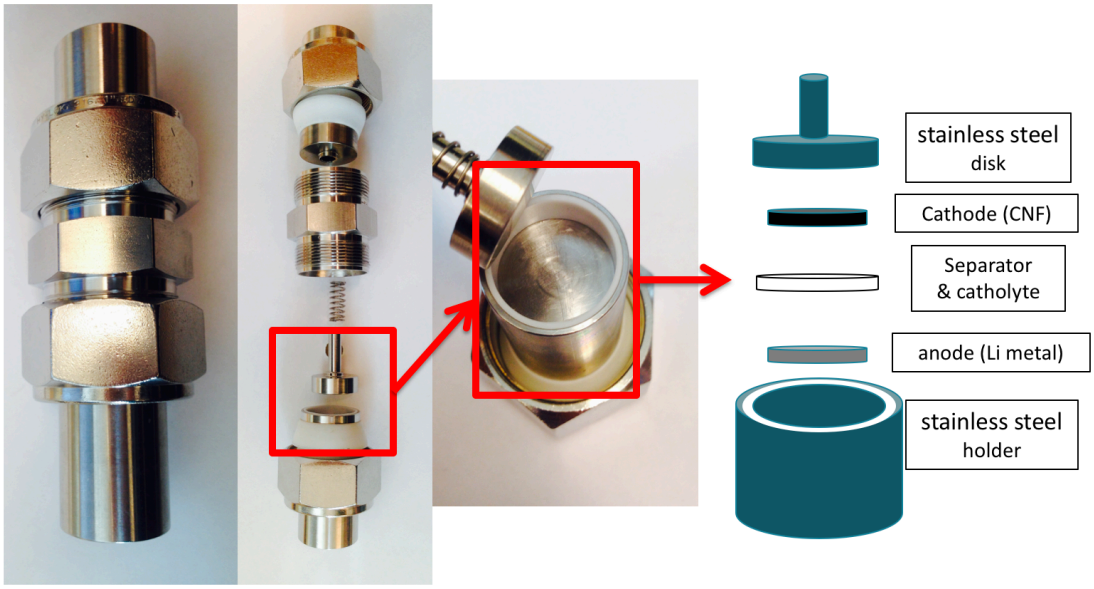

Figure 19. Images of a Swagelok cell, its components and electrode configuration.

Figure 19 shows a Swagelok cell and its components and electrode configuration in the cell. All cells used in this thesis were assembled in an argon-filled glove box. Before assembly all components and the electrodes were dried in vacuum at 60 - 80 °C. It has advantage of easily assembled and disassembled. As this, reusable, good for analysis after cycle and must be cleaned before reuse.

In a typical cell used in this work the cathode, anode and the separator membrane have diameters of 10, 11 and 14 mm, respectively. The separator is usually larger to ensure that there is no contact between anode and cathode. When assembling the cell the sequence outlined figure 19 is followed: 1. lithium metal anode is put on the stainless steel holder and pressed flat, 2. electrolyte is added onto the lithium metal surface, 3. the separator membrane is placed in the cell, 4. electrolyte is added, 5. cathode is placed in the cell.

4.2.2 Cyclic Voltammetry

Cyclic voltammetry (CV) is a potentiodynamic electrochemical method. In the experiment the change in current is determined when cycling the voltage between two limits. CV is often the first electrochemical method to be applied when investigating a new material since the voltage at which different processes are taking place is revealed. Therefore, it is used to characterize charge/discharge reactions as a function of voltage, quantity of charge stored, and reversibility of the reactions or the presence of irreversible reactions [125]. The scan rate can be varied depending on the purpose of the experiment, but for a detailed analysis the scan rate should be low (< 5 mV/s) [126].

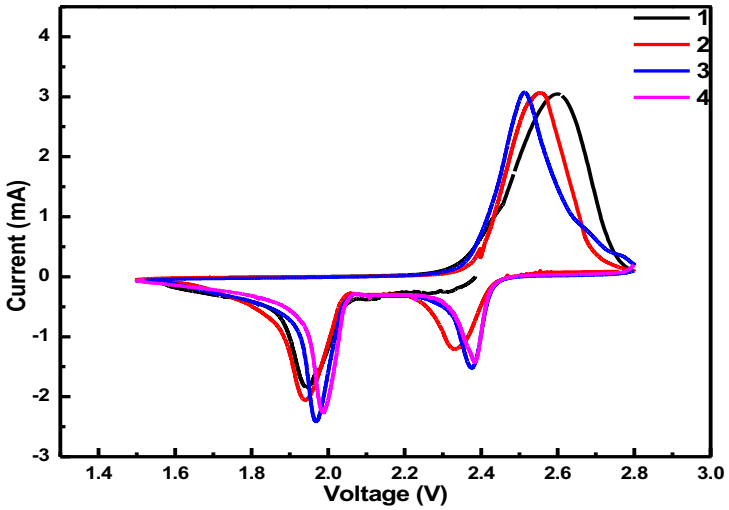

Figure 20. CV curves over 4 cycles of a Li/catholyte/CNF cell between 1.5 to 2.8 V at a scan rate of 0.1 mV/s.

As an example, figure 20 shows the results of a CV experiment on a Li metal/catholyte/CNF cell between 1.5 to 2.8 V. The electrochemical reactions corresponding to the conversion of sulphur to long chain lithium polysulphides and the subsequent conversion to short chain polysulphides at the cathode are the negative peaks (reduction reaction of the Li) and the positive peak corresponds to the conversion in the other direction ideally ending up with elemental sulphur at the cathode (oxidation reaction of the Li). The fact that one only sees one positive peak is that the scan speed is too high and the kinetics relatively slow so that the two peaks have merged into one.

4.2.3 Galvanostatic charge-discharge

In a galvanostatic charge-discharge experiment the specific capacity, reversibility, charge-discharge speed and resistance of the cell can be obtained [127,128]. In this experiment a constant current (CC) is passed to the electrode and the voltage is measured as a function of time. By multiplying the time, it takes for one full discharge (or charge) by the applied current one can calculate the capacity of the cell. Most often the capacity of an electrode investigated will be expressed as a specific capacity, mAh/g with respect to the active material. This value can then be compared to the theoretical capacity to assess the utilization of active material at certain discharge conditions

(discharge rate, temperature, etc). The theoretical capacity of an active material can be calculated from Faraday's Law (Eq. 4.1) [129].

$$\text{Theoretical capacity} = \frac{nF}{3600 \times M} \text{ (mAh/g)} \qquad (4.1)$$

where n, F and M are the number of electrons (released or accepted / molecular unit), Faraday's constant (1F: $(6.023 \times 10^{23}) \times (1.6 \times 10^{-19}\text{C}) = 96{,}487\text{C}$ (1C=1A·s)), and molecular weight, respectively.

In most cases the cell is not full discharged, i.e. down to 0V, but one uses voltage cut-offs. However, for anode materials the constant capacity control is often used since many anode materials deliver a large part of their capacity at voltages close to 0V., see figure 21. For practical applications the rate capability, i.e. the capacity of a cell at certain charge (discharge) rate, is of importance. The rate is commonly expressed in terms of C-rate, where 1 C corresponds to discharging the cell in one hour. A more relevant figure of merit is the capacity at a certain current density (Ag^{-1}) since this also takes into account the loading of the electrode. For an electrode with low active material loading a relatively lower current density is required for a certain C-rate compared to an electrode with high loading. This can be of practical importance since e.g. dendrite growth is known to be more pronounced at high current densities [23].

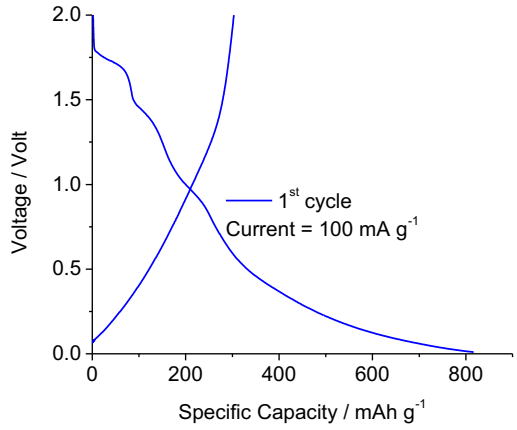

Figure 21. Charge/Discharge voltage profiles of CNF anode half-cell at the first

As an example, figure 22 shows the charge/discharge voltage profiles of a LiS-cell and its cycle performance. From these profiles coulombic efficiency, utilization of electrode material, energy density and the reversibility of the charge-discharge reaction can be determined. The sulphur cathode has a theoretical specific capacity of 1675 mAh/g with respect to sulphur. In figure 21 the specific capacity was determined to 1190 mAh/g at first discharge and the first charge capacity was 1328 mAh/g. Thus, this LiS-cell has Coulombic efficiency of 90 % and active materials utilization is around 70%. From the plot of specific capacity as a function of cycle number we conclude that the reversibility of the reactions is poor since we see a rapid capacity fading. We can also calculate that the average voltage from the discharge curve, in this case 2.1V. From this we can calculate the energy density of the cell (specific capacity x average voltage) of the be 2499 Wh/kg with respect to the weight of sulphur.

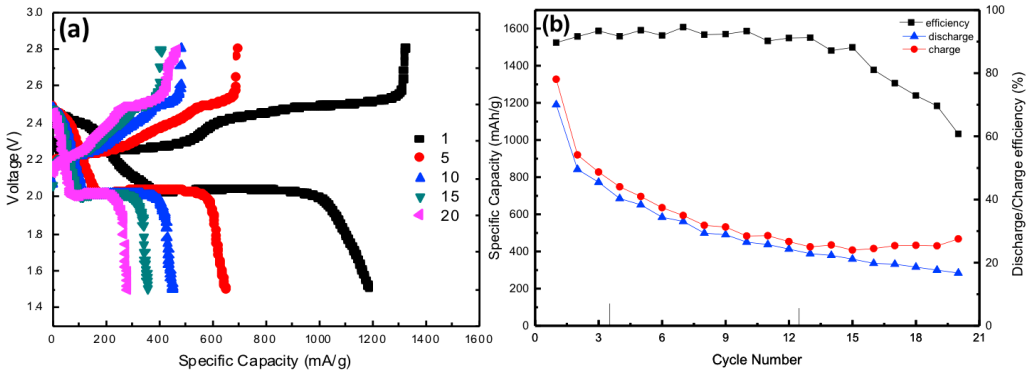

Figure 22. Charge-discharge profiles of a LiS-cell during cycling (a), and cycle performance (b) at 1/16 C.

To more specifically evaluate the stability of the electrolyte and the build-up of SEIs on the Li-anode symmetrical cell tests can be performed. These are very similar to galvanostatic charge-discharge experiment and the voltage is recorded when applying a constant current [130,131]. Figure 23 shows the cycling behaviour of a symmetrical cell of sodium metal with the electrolyte 1M $NaCF_3SO_3$ in PEGDME with PAN membrane at a current density of 0.40 mA/cm^2. Each cycle consists of 15 min charge, 15 min discharge and 5 min rest time between each cycle. In this case we can observe that the voltage is quite low (40 mV) and very stable after 72 h. Thus, the experiment shows that the of gel-polymer electrolyte has a good compatibility with the sodium metal anode and that the resistance is low.

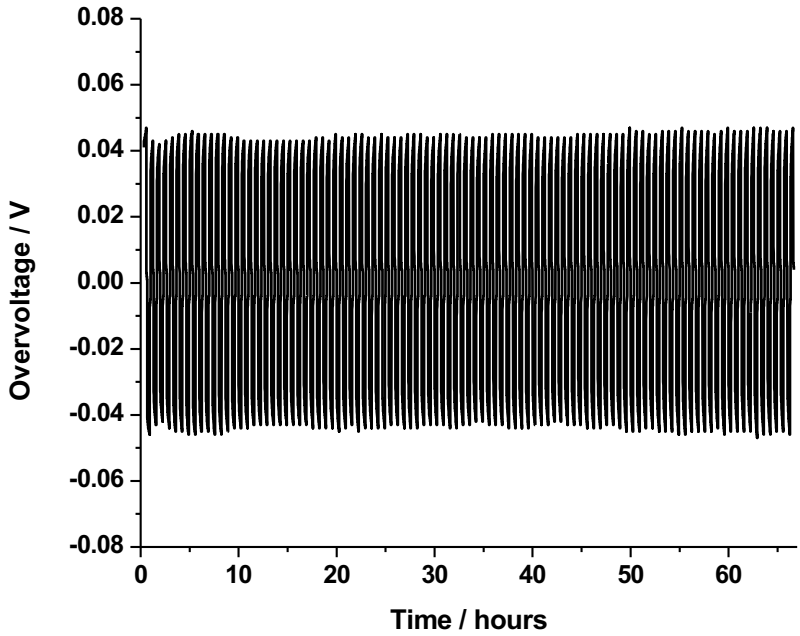

Figure 23. Cycling behaviour of a symmetrical cell with the electrolyte 1M $NaCF_3SO_3$ in PEGDME with PAN membrane.

4.2.4 Impedance Spectroscopy

Impedance spectroscopy is commonly used to investigate the electrode/electrolyte [26,132-135]. From the experiment the resistance and the stability of the interface can for instance be determined. In the experiment a sinusoidal voltage is applied

$$V(t)=V_0 \cdot \sin(\omega t) \qquad (4.2)$$

and the resulting current response is recorded

$$I(t) = I_0 \cdot \sin(\omega t - \theta) \qquad (4.3)$$

where θ is the phase shift. The ratio of the voltage and the current is the impedance and due to the phase shift this is a complex quantity, $Z^*(\omega)=Z'(\omega)+iZ''(\omega)$. The data is commonly presented in the so called Nyquist plot where for each frequency the real and imaginary part of the impedance are plotted, see Figure 24 which schematically shows how a Nyquist plot from an experiment on a Li battery could look.

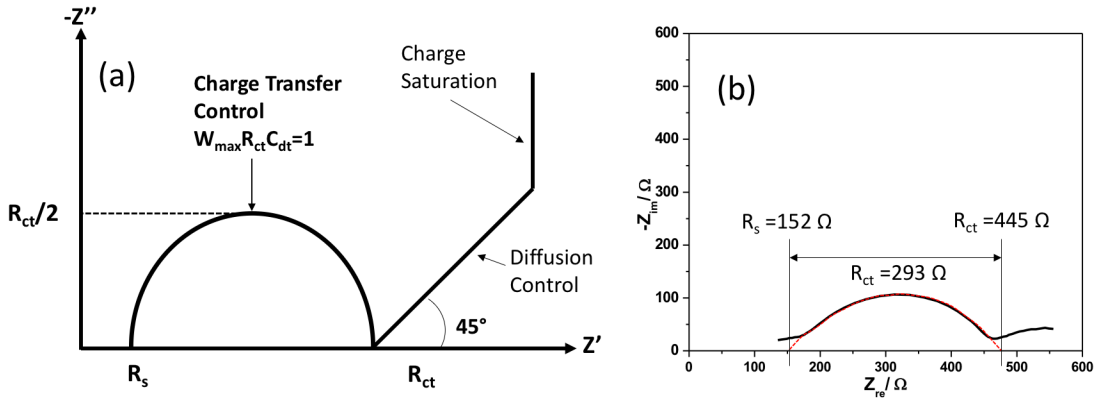

Figure 24. Schematics of the Nyquist plot by equivalent circuit of Li battery (a) and Na/Gel polymer electrolyte/Sulphur cell (b).

The response can be divided into three categories: high frequency, intermediate frequency (Warburg impedance), which is dominated by diffusion, and low frequency which is determined by charge saturation. Figure 24(b) shows an experimental result form an impedance experiment on a Na/Gel polymer electrolyte/Sulphur cell. The points where the semicircle (extrapolated dashed red line) meets the x-axis correspond to R_s and R_{ct} and the resistance of the gel polymer electrolyte sodium cell, between counter electrode and electrolyte, can be determined to 293 Ω. Thus, with this experiment we can following the behaviour of the internal resistance of cell over time and/or for different cycles.

4.3 Physical Characterization

4.3.1 Ionic conductivity

To measure the conductivity of electrolytes an experiment similar to AC impedance is used, i.e. an alternating filed is applied and the complex impedance, $Z^*(\omega)$ is determined. However, to only have the contribution from the conductivity blocking electrodes should be used, i.e. electrodes that do not allow any electrochemical reaction to occur and which are also inert towards the electrolyte. From the complex impedance the complex dielectric function, $\varepsilon^*(\omega)$, can be determined which is related to the conductivity through

$$\sigma(\omega) = i\omega\varepsilon_0\varepsilon''(\omega) \qquad (4.4)$$

From the frequency dependent conductivity the DC conductivity is extracted as the constant plateau value at high frequencies, see Figure 25a. At low frequencies the spectrum is dominated by polarization effects. Typically, the conductivity should be above 10^{-3} S/cm for good performance of a battery. Figure 25b shows the ionic conductivity of a gel polymer electrolyte. From that plot we can determine that in the range 10 to 120 °C the conductivity is sufficient. The kink in the curve observed around 0 °C is due to crystallization of the liquid component which leads to a rapid drop in the conductivity.

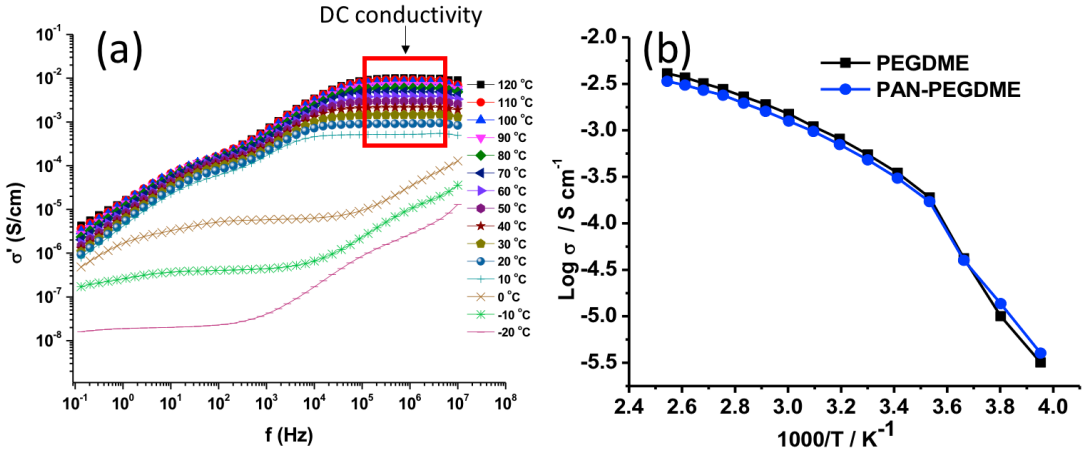

Figure 25. a) Frequency dependent conductivity and b) conductivity as a function of temperature of 1M $NaCF_3SO_3$ in PEGDME with and without PAN membrane. The red square in a) marks the region used for determining the conductivity.

4.3.2 Thermogravimetric analysis (TGA)

In a TGA experiment the mass of a sample is monitored as a function of temperature, or time [136,137]. It is a simple analytical technique primarily used to determine e.g. concentration of water in a sample, loss of solvent, loss of plasticizer, decarboxylation, pyrolysis, or decomposition of the material [26,138]. Figure 26 shows a schematic of a TGA device. It is composed of a sample holder, precision balance, thermocouple and furnace. Normally the experiment is performed under inert atmosphere (e.g. N_2 or Ar) to prevent oxidation or other undesired chemical reactions.

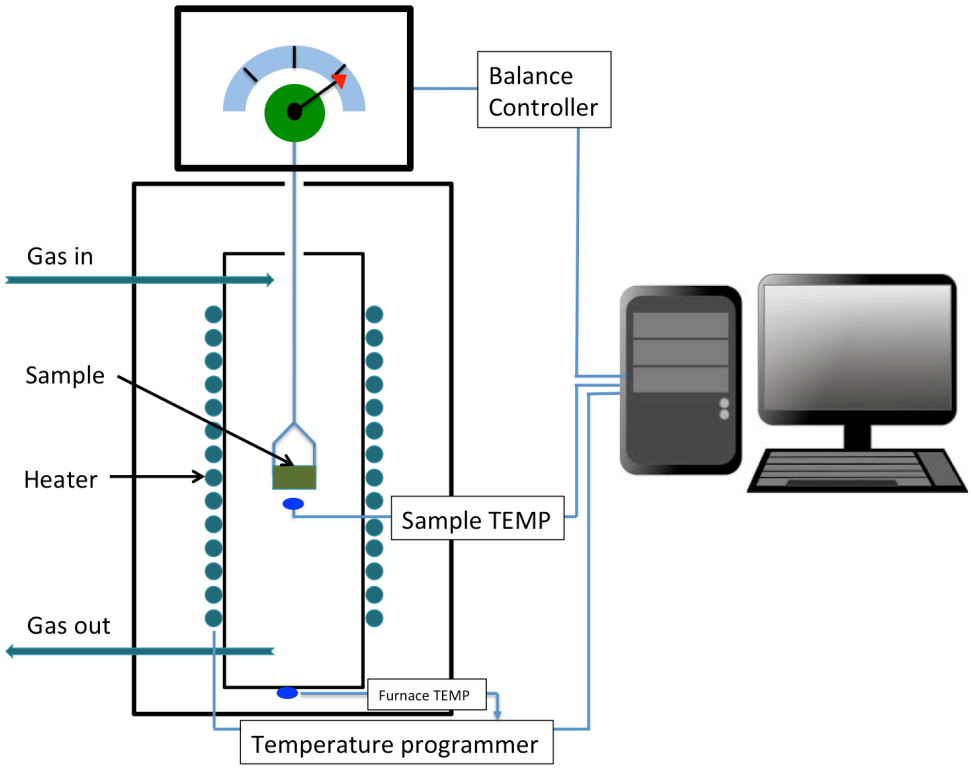

Figure 26. Schematic of a TGA device.

As an example, Figure 27 shows TGA data of a CNF cathode after charge. The aim of this experiment was to determine the amount of Sulphur in/on the CNF membrane after charge of a LiS catholyte cell. From the data one can see that the weight loss occurs in three ranges. The first range (25 - 173 °C) is the loss of the electrolyte, the second range (173 - 264 °C) corresponds to loss of sulphur from the CNF surface and from meso-pores, and the last range (264 - 500 °C) is related to loss of sulphur in micro-pores. Thus, from this TGA data we can determine the content of the different components (sulphur, electrolyte and CNF) in the cathode after charge.

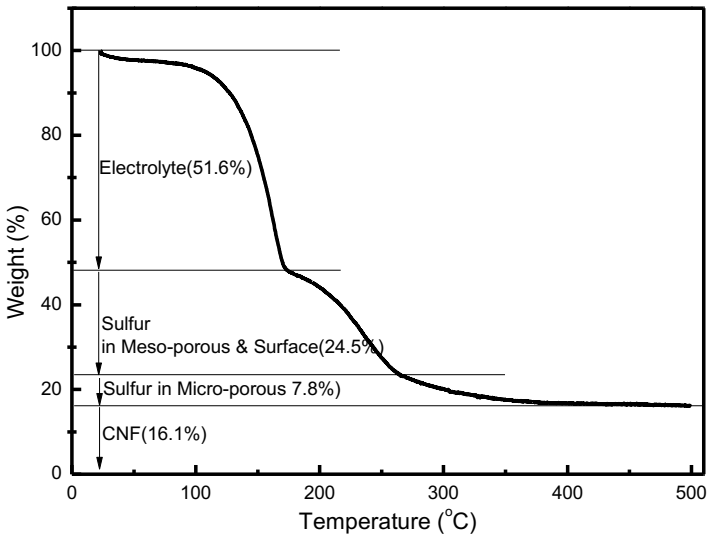

Figure 27. TGA curve of a CNF cathode after charge.

4.3.3 Differential scanning calorimetry (DSC)

Differential scanning calorimetry (DSC) is widely used in materials science to analyse thermal properties of materials. In DSC the difference in the amount of heat required to increase the temperature between a sample and reference (non-reactive substance) is determined and related to physical changes (phase changes) of the sample [139,140]. Figure 28 shows a typical DSC thermogram of a liquid with the three phase transitions that can occur: the glass transition (T_g), crystallization (T_c) and melting (T_m).

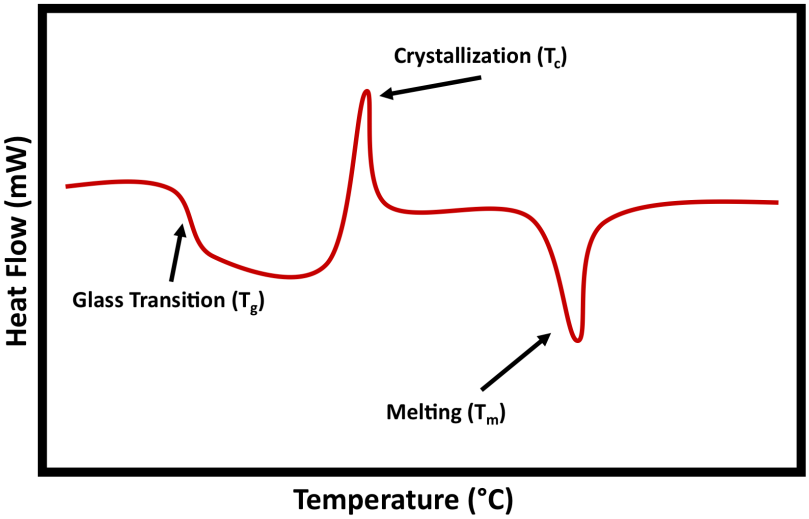

Figure 28. Typical DSC thermogram of a liquid.

Figure 29 shows a schematic of a DSC device. It is composed of a sample, reference, thermocouple and furnace. Normally the experiment is performed under inert atmosphere (e.g. N_2 or Ar) to prevent oxidation or other undesired chemical reactions. The reference has to have a well-known heat capacity and is most commonly an empty pan (Al) is used.

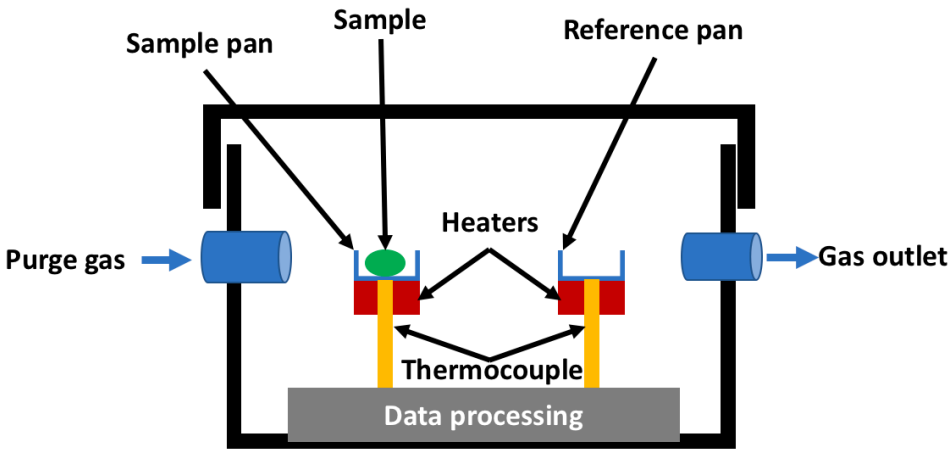

Figure 29. Schematic of a DSC instrument.

5. Summary of Appended Papers

Paper I

Route to sustainable lithium-sulfur batteries with high practical capacity through a fluorine free polysulfide catholyte and self-standing Carbon Nanofiber membranes

In this paper a new concept for a lithium-sulphur battery based on a lithium polysulphide containing electrolyte, a so called catholyte, and an electrospun carbon nano-fibre (CNF) electrode is presented. In contrast to previous reports on catholyte concepts in our approach the lithium polysulphides act both as the conducting Li-salt and as the active material. We show that the conductivity of the catholyte is sufficient and that it can form a stable interface on the Li-metal anode. The key points of the paper is that with this concept we combine high active materials loading, which is the prerequisite for high practical capacity, a metal current collector free design by using the self-supporting CNF cathode, decreasing the overall weight of the cell, and a fluorine free system improving the sustainability.

In the catholyte concept the cathode, in our case the CNF membrane, is sulphur free and is only there to support the electrochemical reactions. To be able to use the high active materials loading provided by the catholyte it is necessary to have high surface area. We use KOH etching to create nm sized (3-4 nm) pores in the fibres which increases the surface area by more than two orders of magnitude. Furthermore, we create larger pores, around 30 nm, by etching away silica nano-particles that were include in the fibres during the preparation by electrospinning. By comparing cells with CNF membranes with and without the larger pores we show that these are important to have a high rate capability, as can be seen in figure 30.

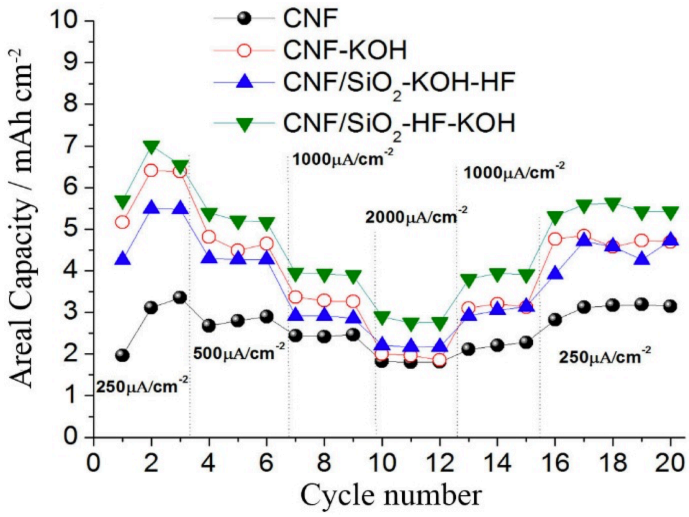

Figure 30. Discharge areal capacity at the various current densities.

Paper II

An electrospun nano-fibre membrane as gel-based electrolyte for room temperature Na/S batteries

Stable cycling of NaS-cells at room temperature is a challenge. Low materials utilization and/or rapid capacity fading is normally observed. The reason for the poor performance is the dissolution of polysulphides in the electrolyte causing side reactions at the Na-metal anode. In this paper we show that the application of a gel polymer electrolyte (GPE) membrane can improve both the specific capacity and the cycling stability compared to a standard separator.

The GPE membrane is prepared by electrospinning of polyacrylonitrile (PAN) and is swollen in a 1M $NaCF_3SO_3$ in polyethylene glycol dimethyl ether (PEGDME, MW=500) solution. The membrane has a high liquid uptake which is a requirement for having a high ionic conductivity, as shown in figure 31. An important feature of this GPE membrane is that it shows a very stable interfacial resistance towards the Na-metal anode. The prototype cell showed stable cycle performance with a specific discharge capacity around 500 mAh/g over 40 cycles.

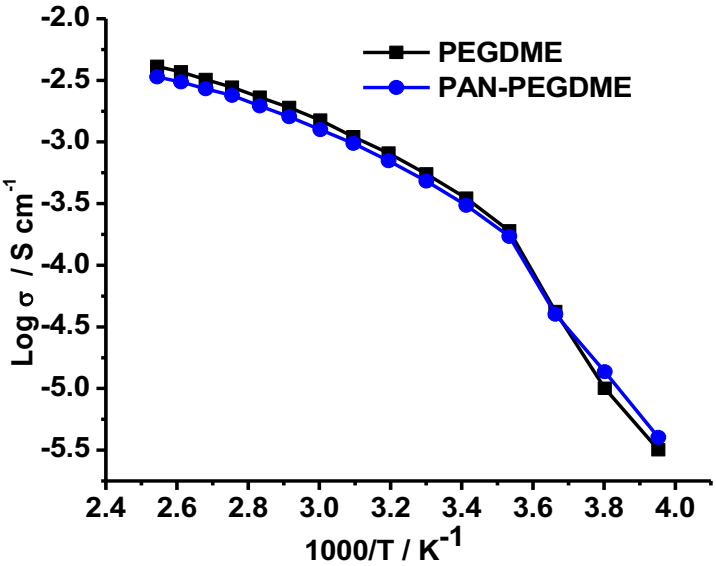

Figure 31. Temperature dependence of the ionic conductivity of pristine PEGDME and PEGDME+PAN in the temperature range −20 °C to 120 °C.

Paper III

Electrospun core-shell nanofiber web as high performance cathode for iron disulfide-based rechargeable lithium battery

Li/FeS_2 cells have theoretically very attractive properties but suffer in practice from a rapid capacity fading. In this paper we present a new cathode material based on the incorporation of FeS_2 in a carbon nano-fibre matrix. This configuration has the advantage of short diffusion paths for ions, large accessibility of active material and a high structural stability. To obtain this structure the precursor FeS_2-PVdF nano-fibre is coated with a layer of sucrose to stabilise the polymer fibre during carbonization avoiding a collapse of the fibre structure, as seen in figure 32. We show that with this configuration a Li/FeS_2 cell can deliver a high specific capacity and a very good rate capability. From the discharge/charge profiles we can also conclude that the reaction mechanism in this cell is a mix between the Li/FeS_2- and the Li/S-electrochemical reactions.

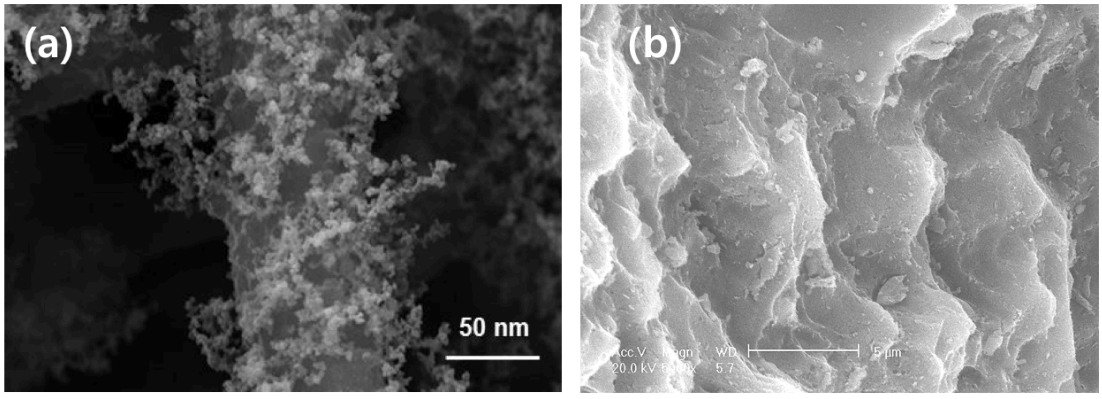

Figure 32. Destruction of fibre morphology with (a) and without (b) additional sucrose coating after carbonization.

Paper IV

Free-standing 3-D sponged nano-fibre electrodes for ultrahigh-rate energy storage devices

We have previously shown how a CNF membrane can be applied as a self-standing cathode in a LiS-cell. In this paper we show that the CNF membrane can also be applied as an anode. The anode is designed at the nanoscale with highly conductive porous carbon fibres with a small diameter enabling short transport distance for lithium-ion diffusion and high electronic conduction in 3D pathways. Thus, it has both a high capacity but, in particular, a very good rate capability. To avoid an irreversible capacity during the first cycles the CNF membrane was pre-cycled in a Li-semi cell configuration for 5 cycles. This process is schematically reported in Figure 33.

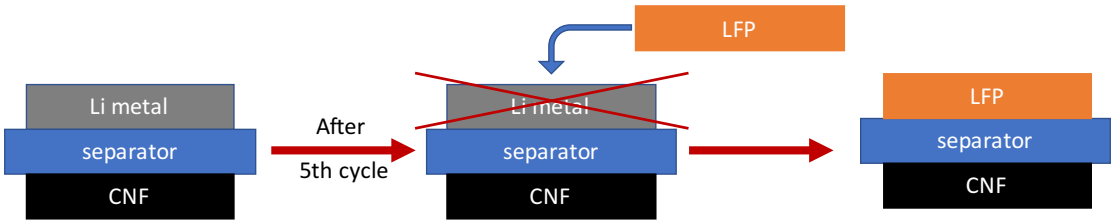

Figure 33. Schematic process for the CNFs full cell assembly. CNFs/Li pre-cycling at 200 mA/g for 5 cycles. Replacement of the Li anode by the use of the LFP cathode.

To demonstrate the applicability of this anode in a Li-battery we coupled it to a LFP-cathode. During the first charge the battery delivers a capacity close to the theoretical value of LFP, 170 mAh/g. However, the process is not fully reversible during the following discharge. This can be ascribed to the stabilization of the cathode and anode materials in the full Li-ion configuration, confirmed also by a low Coulombic efficiency during the first cycles. After 20 cycles the Coulombic efficiency of the cell increases to values close to the 99 %. By the application of this anode in a Li-ion cell we estimate an increase by more than 50 % in energy density and a reduction in cost by removing the need of a Cu current collector.

Paper V

Towards low cost and high energy lithium sulfur batteries through the use of a tailored fluorine-free@Li_2S_8 based electrolyte medium.

CMK3 is one of the classic porous carbon structures used to entrap sulphur for stable cycling in LiS-cells. However, most reports using this material show stable cycling and high specific capacities, but these cells typically have a very low loading and use a high amount of electrolyte (electrolyte/sulphur weight ratio). In this paper, we show that a CMK3/S composite with high sulphur content (78 wt.%) can be combined with a Li_2S_8 catholyte to obtain a LiS-cell with a high active material loading and long cycle life. The total sulphur loading in this cell is 3.6 mg/cm^2 but the amount of electrolyte is only 10 µl/cm^2. We show that the specific capacity is around 800 mAh/g over 500 cycles, see figure 34, considering the total weight of sulphur (in the cathode and in the catholyte). The resulting energy density of the cell is more than 350 Wh/kg and thus meets the requirements for large scale energy storage applications.

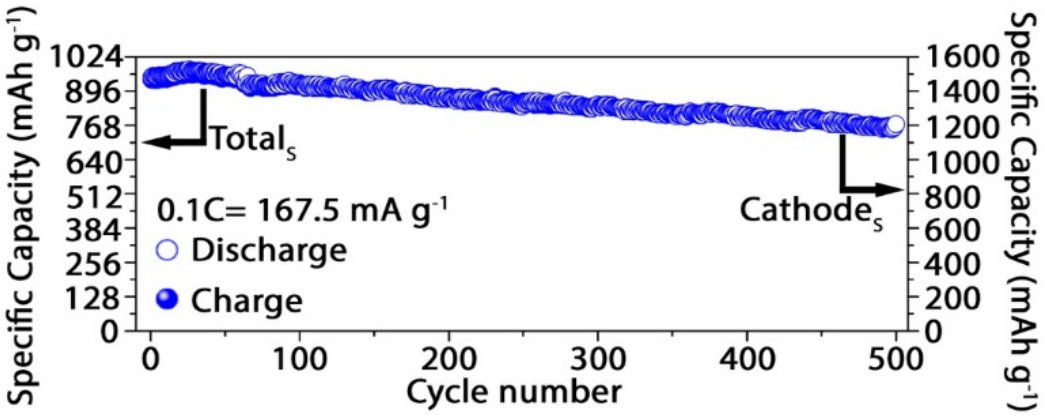

Figure 34. Prolonged cycling performance of the S/CMK3 electrode in Li half cells using DOL-DME $LiNO_3$ 0.4M Li_2S_8 0.5M electrolyte at a current rate of 0.1C.

Paper VI

Stabilizing the Performance of High-Capacity Sulfur Composite Electrodes by a New Gel Polymer Electrolyte Configuration

A solid polymer electrolyte would be very attractive to use in a LiS-cell since it would prevent polysulphide dissolution and mitigate dendrite formation at the Li-metal anode. However, polymer electrolytes typically suffer from a low conductivity at room temperature and high interfacial resistance towards the electrodes. To circumvent these issues, we propose to use a gel-polymer electrolyte, based in a PVdF-membrane swollen in a 1 m LiTFSI & 0.4 m $LiNO_3$ in DOL/DME (1:1 v/v) solution, which combines the mechanical rigidity of the polymer with the high conductivity and wettability of a liquid electrolyte. We demonstrate this concept by combining the gel-polymer electrolyte membrane with a rather simple sulphur/carbon composite cathode. In figure 35 the discharge/charge voltage profiles for a cell using the gel-polymer electrolyte membrane is compared to a cell with a standard Whatman (glass fibre) separator. It is clear that the cell with the gel-polymer electrolyte membrane has a much higher cycling stability and delivers a very high specific capacity for more than 100 cycles. However, it is also clear that the voltage profiles are quite different, which is most likely related to the different dissolution properties resulting in different polysulphide speciation and these electrochemical reactions.

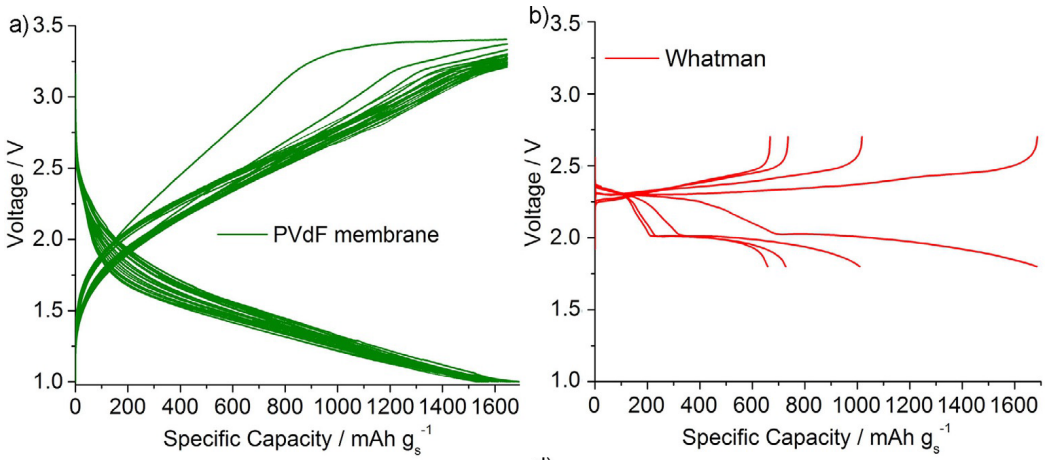

Figure 35. Galvanostatic voltage profiles of Li–S cells using a) the GPE and b) the Whatman membrane.

6 Summary and Outlook

The focus of this work has been to take one step towards the realisation of LiS-batteries in practice. The principle of the technology has been known for many years but so far LiS-cells have either a short cycle life or a very low energy density. In recent years there has been an increased interest in the direction of LiS-cells with a high loading of active material and still good cycle life and high active material utilization, i.e. specific capacity. My work has been part of these efforts and it has also included how to improve sustainability aspects and also considering cost.

As results of this work several concepts for cells based on the conversion of sulphur are presented. Two of the main topics have been to work with a catholyte, which both stabilises the cycling and contributes to increasing the active material loading, and to work with electrospun materials, which enable to obtain self-supporting structures and/or to tailor the morphology on the nanoscale. These approaches have been combined with developing fluorine free cells and a NaS-cell with good performance at room temperature. Both these developments contribute to both improvement of sustainability and in terms of cost. Major results of the work are:

- the use of catholytes without a traditional Li-salt and where the added polysulphides are both conducting agent and active material in high capacity cells.
- the use of free standing electrodes based on highly conducting carbon nano-fibre membranes. This configuration does not require the use of a metal current collector which reduces the overall weight of the cell
- showing that a gel-polymer electrolyte membrane can stabilise the interface of a Na-metal anode leading to stable cycling of a NaS-cell at room temperature
- that LiS-cells with a very low amount of electrolyte with respect to active material can be realised by the application of a catholyte to a high loading CMK3/S cathode resulting in a high energy density cell

Even though the results from this thesis have helped us to take one step in the right direction there is still some way to go before one can bring these concepts to the market or even to a prototype. A key point will be to even in more detail investigate and fully understand the processes involved in for instance the catholyte cells or in the cells with a gel-polymer electrolyte membrane where the discharge curve shows a quite different voltage profile compared to a cell with a traditional separator. To obtain such understanding more systematic studies of the phenomena are needed especially during operation. So far, the characterization has been made mostly ex-situ and the next step would be to study the materials directly in a working cell by for instance Raman spectroscopy or x-ray diffraction. Another aspect to explore for the future is if the successful CNF and catholyte concepts for LiS-cells can be transferred to NaS-cells. With lithium prices rising steeply as lithium reserves decline the transfer to Na-technology is very important. Decreasing the cost and having truly sustainable batteries is crucial for implementation in large scale applications and for our transition to a sustainable society.

Acknowledgements

Firstly, I would like to thank my supervisors professor Aleksandar Matic and Per Jacobsson, for your advice, your assistance and giving me the opportunity to study at Chalmers.

Thanks to all at KMF for discussions and being helpful, and I would like to thank Ezio Zanghellini for support every time I asked for help and Marco Agostini for a lot of support on the work on my papers and my thesis.

I would like to thank professor Jou-hyeon Ahn who was my supervisor when I was a master student, and who has continuously been giving me help and advice. Thanks also to Dr. James Manuel who was co-author of my papers and gave me lots of help.

Finally, I would like to give respectful thanks to my parents. They always stand by me in joy and sorrow. Specially thanks to my wife (Yongju) for alone taking care of our son in Korea during the preparation of my thesis, she is very understanding about my goals and always supports me. I am thankful to see that my son (Haejun) is healthy and I want everyone to be happy.

Bibliography

[1] M. Ikoma, N. Fujioka, Kagaku Kogyo 49 (1998) 45

[2] T. Nagura and K. Tazaawa, Prog. Batteries Sol. Cells 9 (1990) 20.

[3] J.Hassoun, S.Panero, P. Reale, B. Scrosati, Adv. Mater. 21 (2009) 2809

[4] E. Karden, S. Ploumen, B. Fricke, T. Miller, K. Snyder, J. Power Sources 163 (2007) 2.

[5] J.W. Fergus, J. Power Sources 195 (2010) 939

[6] B. Xu, D. Quian, Z. Wang, Y.S. Meng, Mater. Sci. Eng. R 73 (2012) 51.

[7] G.A. Nazri, G. Pistoia, (Eds), "Lithium batteries: Science and Technology", Kluwer Academic Publishers, New York (2004) 350.

[8] J. Shim, K.A. Striebel, E.J. Cairns, J. Electrochem. Soc. 149 (2002) A1321.

[9] J. Wang, L. Liu, Z. Ling, J. Yang, C. Wan, C. Jiang, Electrochim. Acta 48 (2003) 1861.

[10] H.S. Ryu, J.W. Choi, J.H. Ahn, G.B. Cho, H.J. Ahn, Mater. Sci. Forum 510-511 (2006) 50.

[11] J.W. Choi, J.H. Kim, G. Cheruvally, J.H. Ahn, K.W. Kim, H.J. Ahn, J.U. Kim, J. Ind. Eng. Chem. 12 (2006) 939.

[12] E. Peled, Y. Sternberg, A. Gorenshtein and Y. Lavi, J. Electrochem. Soc. 136 (1989) 1621.

[13] J.O. Besenhard, Handbook of Battery Materials, Wiley, New York (1999).

[14] P.G. Bruce, Chem. Commun. 19 (1997) 1817.

[15] M. Armand et al. U.S Patent No. US745701B2

[16] A. K. Padhi, K.S. Nanjundaswamy, J.B. Goodenough, J. lctrochem. Soc. 144 (1997) 1188

[17] A. Yamada, S. C. Chung, K. Hinokuma, J. Electrochem. Soc. 148 (2001) A224

[18] L. P. L. M. Rabou, A. Roskam, J. Power Sources, 54 (1995) 316.

[19] R. Yazami, N. Lebrun, M. Bonneau, M. Molteni, J. Power Sources 54 (1995) 389.

[20] C. Y. Yao, T. H. Kao, C. H. Cheng, J. M. Chen, W. M. Hurry, J. Power Sources 54 (1995) 491.

[21] T. Nohma, H. Kurokawa, M. Uehara, M. Takahashi, K. Nishio, T. Saito, J. Power Sources 54 (1995) 522.

[22] J. Kim, D. Kim, D. Lim, A. Matic, G. S. Chauhan, J. Ahn, Solid State Ionics 262 (2014) 25–29

[23] M. Agostini, S. Xiong, A. Matic and J. Hassoun, Chem. Mat. 27 (2015) 4604-4611

[24] Y. Tang, L. Yang, S. Fang, Z. Qiu, Electrochimica Acta 54 (2009) 6244–6249

[25] T Ohzuku, A. Ueda, N. Yamamota, J. Electrochem. Soc. 142 (1995) 1431-1435

[26] J.G. Park, Principles and applications of lithium secondary batteries, Hongrung publishing company (2010).
[27] H. Lee, Y. Wang, C. Wan, M. Yang, H. Wu, D. Shieh, Journal of Applied Electrochemistry 35 (2005) 615–623
[28] M. Agostini, Y. Aihara, T. Yamada, B.Scrosati, J. Hassoun, Solid State Ionics 244 (2013) 48-51
[29] T. Yamada, S. Ito, R. Omoda, T.atanabe, Y. Aihara, M. Agostini, U. Ulissi, J. Hassoun, B. Scrosati, Journal of The Electrochemical Society 162 (2015) 646-A651
[30] P.G. Bruce, S.A. Freunberger, L.J. Hardwick, J.M. Tarascon, Nature Materials 11 (2012) 19
[31] http://www.nissanusa.com/leaf-electric-car/specs-features/index#/leafelectric-car/specs-features/index.
[32] A. Taniguchi, N. Fujioka, M. Ikoma, A. Ohta, Journal of Power Sources 100 (2001) 117-124
[33] US Advanced Battery Consortium USABC Goals for Advanced Batteries for EVs (2006). Available at: http://uscar.org/commands/files_download.php?files_id=27.
[34] G.A. Nazri, G. Pistoia, (Eds), “Lithium batteries: Science and Technology”, Kluwer Academic Publishers, New York, (2004) 350.
[35] E Peled, Y. Sternberg, A. Gorenshtein, Y. Lavi, J. Electrochem. Soc. 136 (1989) 1621.
[36] D.Marmorstein, T.H. Yu, K.A. Striebel, F.R. Mclarnon, J. Hou, E.J. Cairns, J Power Sources 89 (2000) 219.
[37] N. Cañas, S. Wolf, N. Wagner, K. Friedrich, Journal of Power Sources 226 (2013) 313-319
[38] S. Zhang, J. ReadJournal of Power Sources 200 (2012) 77– 82
[39] N. Cañas, S. Wolf, N. Wagner, K. Friedrich, Journal of Power Sources 226 (2013) 313-319
[40] Y. Fu, C. Zu, A. Manthiram, J. Am. Chem. Soc. 135 (2013) 18044−18047
[41] B. Kim, S. Park, J. Electrochem. Soc. 140 (1993) 115–122
[42] R. Demir-Cakan, M. Morcrette, Gangulibabu, A. Gueguen, R. Dedryveredb, J. Tarascon, Energy Environ. Sci. 6 (2013) 176
[43] N. Manan, L. Aldous, Y. Alias, P. Murray, L. Yellowlees, M. Lagunas, C. Hardacre. The journal of physical chemistry. B 115 (2011) 13873–9
[44] B.D. Katz, L.C. Dejonghe, M.Y. Chu, S.J. Visco, U.S. Patent No.6,200,704 B1 (2001)
[45] J.L. Wang, J.Yang, J.Y. Xie, N.X. Xu, Y. Li, Electrochem. Commun. 4 (2002) 499
[46] Y.V. Mikhaylik, J.R. Akridge, J. Electrochem. Soc. 151 (2004) A1969.
[47] L.X. Miao, W.K Wang, A.B. Wang, H.G. Yuan, Y.S. Yang, J. Mater. Chem. A 1 (2013) 11659.
[48] D. Bresser, S. Passerini, B. Scrosati, Chem. Commun. 49 (2013) 10545

[49] X. Ji, K. Lee, L. Nazar, Nature Mater. 8 (2009) 500.
[50] H. j. Choi, X. Zhao, D.S. Kim, H.J. Ahn, K.W. Ki, K.K. Cho, J.H. Ahn, Materials Research Bulletin 58 (2014) 199.
[51] J. Kim, D. Lee , H. Jung , Y. Sun, J. Hassoun, B. Scrosati, Adv. Funct. Mater. 23 (2013) 1076–1080
[52] L. Ni, G. Zhao, Y. Wang, Z. Wu, W. Wang, Y. Liao, G. Yang, G. Diao Chem. Asian J. 12 (2017) 3128 – 3134
[53] L. Xiao, Y. Cao, J. Xiao, B. Schwenzer, M.H. Engelhard, L.V. Saraf, Z. Nie, G.J. Exarhos, J. Liu, J. Mater. Chem. A 1 (2013) 9517.
[54] X. Zhao, J.K. Kim, H.J. Ahn, K.K. Cho and J.H. Ahn, Electrochim. Acta 109 (2013) 145.
[55] W. Zhou, Y. Yu, H. Chen, F.J. DiSalvo and H.D. Abruna, J. Am. Chem. Soc. 135 (2013) 16736.
[56] J. Wang, J Yang, C. Wan, K. Du, J. Xie, N. Xu, Adv. Funct. Mater. 13 (2003) 487
[57] J.L. Wang, J. Yang, J.Y. Xie, N.X. Xu, Y. Li, Electrochemistry Communications 4 (2002) 499-502
[58] S. Zhang, Journal of Power Sources 231 (2013) 153-162.
[59] J. Gao, M.A. Lowe, Y. Kiya, H.D. Abruna, J. Phys. Chem. C 115 (2011) 25132-25137.
[60] Y. Mikhaylik, I. Kovalev, R. Schock, K. Kumaresan, J. Xu, J. Affinito, ECS Trans. 25 (2010) 23-34.
[61] N. Ding, L. Zhou, C. Zhou, D. Geng, J. Yang, S. Chien, Z. Liu, M. Ng, A. Yu, T. Hor, M. Sullivan, Y. Zong, Scientific Reports 6 (2016) 33154
[62] [50] T. Jaumann, J. Balach, M. Klose, S. Oswald, J. Eckert, L. Giebelera, Journal of The Electrochemical Society 163 (2016) A557-A564
[63] M. Galiński, A. Lewanddowski, I. Stepniak, Electrochim. Acta 51 (2006) 5567–5580,
[64] L.X. Yuan, J.K. Feng, X.P. Ai, Y.L. Cao, S.L. Chen, H.X. Yang, Electrochem. Comm. 8 (2006) 610–614
[65] J. Scheers, S. Fantini, P. Johansson, J. Power Sour. 255 (2014) 204–218.
[66] S. Xiong, J. Scheers, L. Aguilera, D. Lim, K. Xie, P. Jacobsson, A. Matic, RSC Adv. 5 (2015) 2122
[67] J. Kim, Materials Letters 187 (2017) 40–43
[68] H. Ryu ,C. Park, W. Shin, T. Kim, J. Lee, H. Ahn, Materials Science Forum 486 (2005) 634-637
[69] S. Kang, X. Zhao, J. Manuel, H. Ahn, K. Kim, K. Cho, J. Ahn, Phys. Status Solidi. A 211 (2014) 1895–1899
[70] S. Chen, F. Dai, M. L. Gordin, D. Wang, RSC Advances 3 (2013) 3540
[71] S.S. Zhang, J.A. Read, J Power Sources 200 (2012) 77.
[72] M. Agostini, D.J. Lee, B. Scrosati, Y.K. Sun, J. Hassoun, J. Power Sources 265 (2014) 14.
[73] S. Chen, F. Dai, M.L. Gordin, D. Wang, RSC Adv. 3 (2013) 3540

[74] R. Demir-Cakan, M. Morcrette, Gangulibabu, A. Gueguen, R. Dedryvere, J.M. Tarascon, Energy Environ. Sci. 6 (2013) 176
[75] G.E. McManis, M.H. Miles, A.N. Fletcher, J. Electrochem. Soc.131 (1984) 286.
[76] D.G. Oei, Inorganic Chemistry 12 (1973) 2,
[77] W.L. Bowden, L.H. Barnette, D.L. DeMuth, J. Electrochem. Soc. 135 (1988) 1
[78] S.S. Zhang, D.T. Tran, J Power Sources 211 (2012) 169.
[79] S.S. Zhang, Electrochimica Acta 70 (2012) 344
[80] A. Rosenman, R. Elazari, G. Salitra, E. Markevich, D. Aurbach, A. Garsuchb, J. Electrochem. Soc. 162 (2015) A470
[81] C. Barchasz, J.C. Lepretre, S. Patoux, F. Alloin, J. Electrochem. Soc. 160 (2013) A430.
[82] X. Yu, S. Feng, M. J. Boyer, M. Lee, R. C. Ferrier Jr., N. A. Lynd, G. S. Hwang, G. Wang, S. Swinnea, A. Manthiram, Materials Today Energy 7 (2018) 98-104
[83] X. Zhao, D.S. Kim, J. Manuel, K.K. Cho, K.W. Kim, H.J. Ahn, J.H. Ahn, Cite this: J. Mater. Chem. A. 2 (2014) 7265.
[84] S. Moon, Y.H. Jung, W.K. Jung, D.S. Jung, J.W. Choi, D.K. Kim, Adv. Mater. 25 (2013) 6547.
[85] Y. Zhang, Y. Zhao, A. Yermukhambetova, Z. Bakenov, P. Chen, J. Mater. Chem. A. 1 (2013) 295.
[86] F. Nitze, M. Agostini, F. Lundin, A. E. C. Palmqvist, A. Matic, C. Chang, A. Manthiram, ACS Energy Lett. 3 (2018) 72
[87] C. Chang, A. Manthiram, ACS Energy Lett. 3 (2018) 72−77
[88] D. Lim, M. Agostini, F. Nitze, J. Manuel, J. Ahn, A. Matic, Scientific Reports 7 (2017) 6327
[89] S. Xin, Y-X. Yin, Y-G. Guo, L.-J. Wan, Advance Materials, 26 (2014) 1261
[90] J.L. Sudworth, A.R. Tilley, 'Sodium sulfur battery' Chapman & Hall, New York (1985).
[91] I. Bauer, M. Kohl, H. Althues, S. Kaskel, Chemical communications 50 (2014) 3208-3210
[92] S. Wenzel, H. Metelmann, C. Raiß, A.K. Dürr, J. Janek, P. Adelhelm, Journal of Power Sources 243 (2013) 758-765
[93] H. Ryu, T. Kim, K. Kim, J.-H. Ahn, T. Nam, G. Wang, H.-J. Ahn, Journal of Power Sources 196 (2011) 5186-5190
[94] I. Kim, J. Park, C. Kim, J. Park, J. Ahn, J. Ahn, K. Kim, H. Ahn, Journal of The Electrochemical Society 163 (2016) A611-A616
[95] N. Tanibata, M. Deguchi, A. Hayashi, M. Tatsumisago, Chem. Mater. 29 (2017) 5232−5238
[96] S. K. Park, J. Lee, S. Bong, B. Jang, K. D. Seong, Y. Piao, ACS Appl. Mater. Interfaces 8 (2016) 19456-19465

[97] J. Guo, H. Zhu, Y. Sun, L. Tang, X. Zhang, J. Mater. Chem. A 4 (2016) 4783-4789
[98] L. Yu, J. F. Yang, X. W. Lou, Angew. Chem. Int. Ed. Engl. 55 (2016) 13422-13426
[99] Y. Xiao, J. Y. Hwang, I. Belharouak, Y. K. Sun, Nano Energy 32 (2017) 320-328
[100] H. Pang, W. Sun, L. P. Lv, F. Jin, Y. Wang, J. Mater. Chem. A 4 (2016) 19179-19188
[101] Z. Hu, K. Zhang, Z. Zhu, Z. Tao, J. Chen, J. Mater. Chem. A 3 (2015) 12898
[102] Y. Long, J. Yang, X. Gao, X. Xu, W. Fan, J. Yang, S. Hou, Y. Qian, ACS Appl. Mater. Interfaces 10 (2018) 10945−10954
[103] Y. Zhu, X. Fan, L. Suo, C. Luo, T. Gao, C. Wang, ACS Nano 10 (2016) 1529-1538
[104] F. Rosamada, J.R. Dahn, C.H.W. Jones J. Electrochem. Soc. 136 (1989) 3206-3210
[105] L.A. Montoro, J.M. Rosolen J.H. Shin, S. Passerini , Electrochimica Acta 49 (2004) 3419–3427
[106] L.A. Montoro, J.M. Rosolen, Solid State Ionics 159 (2003) 233-240
[107] D. Golodnitsky, E. Peled, Electrochim. Acta 45 (1999) 335-350
[108] X. Wen, X. Wei, L. Yanga, P. Shen, J. Mater. Chem. A 3 (2015) 2090
[109] T. S. Yoder, M. Tussing, J. E. Cloud, Y. Yang, Journal of Power Sources 274 (2015) 685-692
[110] P. Tsai, H. Gibson, P. Gibson, J. Electrostatics. 54 (2002) 333
[111] H. Jia, G. Zhu, B. Vugrinovich, W. Kataphinan, D. Reneker, P. Wang, Biotechnol. Prog. 18 (2002) 1027
[112] X. Wang, Y. Kim, C. Drew, B. Ku, J. Kumar, L. Samuelson, Nano Lett. 4 (2004) 331
[113] I. Chronakis, S. Grapenson, A. Jakob, Polymer 47 (2006) 1597
[114] D. Lim, J. Manuel, J. Ahn, J. Kim, P. Jacobsson, A. Matic, J. Ha, K. Cho, K. Kim. Solid State Ionics 225 (2012) 631-635
[115] P. Raghavan, X. Zhao, H. Choi, D. Lim, J. Kim, A. Matic, P. Jacobsson, C. Nah, J. Ahn 262 (2014) 77-82
[116] J. Manuel, Y. Liu, M. Lee, X. Zhao, M. Kim, G. Chauhan, H. Ahn, J. Ahn, Science of Advanced Materials 8 (2016) 741-748
[117] D. Zhu, C. Xu, N. Nakura, M. Matsuo, Carbon 40 (2002) 363.
[118] M. Wu, Q. Wang, K. Li, Y. Wu, H. Liu, Polymer Degradation and Stability 97 (2012) 1511.
[119] B. Saha, G. Schatz J. Phys. Chem. B. 116 (2012) 4684−4692
[120] J. Wang, S. Kaskel, J. Mater. Chem. 22 (2012) 23710
[121] J. Liua, Z. Xiong, S. Wang, W. Cai, J. Yang, H Zhang, Electrochimica Acta 210 (2016) 171–180
[122] S. Bhoyate, P. K. Kahol, B. Sapkota, S. R. Mishra, F. Perez, R. K. Gupta, Surface & Coatings Technology 345 (2018) 113–122

[123] H. Tavanai, R. Jalili, M. Morshed, Surf. Interface Anal. 41 (2009) 814–819
[124] J. Li, S. Su, L. Zhou, V. Kundrat, A. M. Abbot, F. Mushtaq, D. Ouyang, D. James, D. Roberts, H. Ye, Journal of Applied Physics 113 (2013) 024313
[125] J. Wang, Analytical Electrochemistry, 3rd Ed., Wiley-VCH (2006).
[126] C.M.A. Brett, A.M.O. Brett, Electroanalysis, Oxford Univeraity Press (1998)
[127] D. McMullan, J. Scanning microscopies 17 (1995) 175.
[128] K.N. Jung, S.I. Pyun, electrchim. Acta 52 (2007) 5453
[129] C.H. Hamann, A. Hammett, W. Vielsich, Electrochemistry, published by Wiley-VCH (1998)
[130] G. Lane, A. Best, D. MacFarlane, M. Forsyth, A. Hollenkamp, Electrochim. Acta. 55 (2010) 2210-2215
[131] S. Xiong, K. Xie, Y. Diao, X. Hong, Journal of Power Sources 246 (2014) 840-845
[132] M. Orazem, B. Trobollet, Electrochemical Impedance Spectroscopy, Wiley (2008)
[133] J. Scully, D. Silverman, M. Kendig, Electrochemical Impedance: Analysis and interpretation, American Soc. for Testing and Materials (1993)
[134] R. White-J.O'M. Bockris-B.E. Conway, Modern Aspects of Electrochemistry, Kluwer Academic Plenum Publishers Chap. 2 (1999) 32
[135] E. Barsoukov, J. Macdonald, Impedance Spectroscopy, 2nd ed., Wiley-Interscience (2005)
[136] P.J. Haines, Principles of thermal analysis and calorimetry, Royal Society of Chemistry (2002).
[137] Y.B. Kim, S.J. Song, Polymer science & technology 4 (1993) 387.
[138] N.A. Tikhonov, I.V. Arkhangelsky, S.S. Belyaev, A.T. Matveev, Thermochimica Acta 486 (2009) 66.
[139] D.A. Skoog, F.J Holler, T. Nieman, Principles of Instrumental Analysis. New York. 805–808 (1998)
[140] G. Höhne, W. Hemminger, H.-J. Flammersheim, Differential Scanning Calorimetry, published by Springer (1996).